

Behind-the-Meter Storage

Anthony Burrell

National Renewable Energy Laboratory
15013 Denver West Parkway
Golden, CO 80401
Phone: (303) 384-6666
E-mail: anthony.burrell@nrel.gov

Samuel Gillard, DOE-EERE-VTO

Technology Manager, Battery R&D
Phone: (202) 287-5849
E-mail: samuel.gillard@ee.doe.gov

Start Date: 1 October 2018

End Date: 30 September 2022

Table of Contents

	Page
Overview	1
BTMS Analysis: Electric Vehicle and Building Load Profiles	4
BTMS Testing and Protocols	21
Power Electronics for Behind-the-Meter Storage	28
BTMS Materials Development	34

Project Introduction

This initiative, referred to as Behind-the-Meter Storage (BTMS), will focus on novel critical-materials-free battery technologies to facilitate the integration of electric vehicle (EV) charging, solar power generation technologies, and energy-efficient buildings while minimizing both costs and grid impacts. For extreme fast-charging at levels of 350 kW or higher, novel approaches are required to avoid significant negative cost and resiliency impacts. However, it is reasonable to assume that BTMS solutions would be applicable to other intermittent renewable energy generation sources or short-duration, high power-demand electric loads. BTMS research is targeted at developing innovative energy-storage technology specifically optimized for stationary applications below 10 MWh that will minimize the need for significant grid upgrades. Additionally, avoiding excessive high-power draws will eliminate excess demand charges that would be incurred during 350-kW fast-charging using current technologies. The key to achieving this is to leverage battery-storage solutions that can discharge at high power but be recharged at standard lower power rates, acting as a power reservoir to bridge to the grid and other on-site energy-generation technologies such as solar photovoltaics (PV), thereby minimizing costs and grid impacts. To be successful, new and innovative integration treatments must be developed for seamless interaction between stationary storage, PV generation, building systems, and the electric grid.

Key components of BTMS will address early-stage research into new energy-generation and building-integration concepts, critical-materials-free battery energy-storage chemistries, and energy-storage designs

with a focus on new stationary energy-storage strategies that will balance performance and costs for expanded fast-charging networks while minimizing the need for grid improvements.

Objectives

A cohesive multidisciplinary research effort to create a cost-effective, critical-materials-free solution to BTMS by employing a whole-systems approach will be taken. The focus of this initiative is to develop innovative battery energy-storage technologies with abundant materials applicable to EVs and high-power charging systems. Solutions in the 1–10 MWh range will eliminate potential grid impacts of high-power EV charging systems as well as lower installation costs and costs to the consumer.

Although many lessons learned from EV battery development may be applied to the BTMS program, the requirements for BTMS systems are unique—carrying their own calendar-life, cycle-life, and cost challenges. For example, EV energy-storage systems need to meet very rigorous energy-density and volume requirements to meet consumer transportation needs. Despite that, current stationary storage systems use batteries designed for EVs due to high volumes that drive down costs. This creates another market demand for EV batteries, further straining the EV battery supply chain and critical-material demand.

By considering BTMS electrochemical solutions optimized for these applications with less focus on energy density in mass and volume, the potential for novel battery solutions is very appealing. Furthermore, the balance-of-plant (BOP) for a BTMS battery system—or, the cost of everything minus the battery cells—is thought to be upwards of 60% of the total energy-storage system cost. In contrast, the EV's BOP costs make up roughly 30% of the total battery cost. Therefore, BTMS will also need to focus on reducing BOP cost through system optimization to realize desired cost targets.

The design parameters are needed to optimize the BTMS system for performance, reliability, resilience, safety, and cost.

The objectives for the project are to:

- Produce BTM battery solutions that can be deployed at scale and meet the functional requirement of high-power EV charging.
- Use a total-systems approach for battery storage to develop and identify the specific functional requirements for BTMS battery solutions that will provide novel battery systems in the 1–10-MWh range at \$100/kWh installed cost—and able to cycle twice per day, discharging for at least 4 hours, with a lifetime of roughly 20 years or at least 8,000 cycles.

Approach

A cohesive multidisciplinary research effort—involving the National Renewable Energy Laboratory (NREL), Idaho National Laboratory (INL), Sandia National Laboratories (SNL), and Argonne National Laboratory (ANL)—will create a cost-effective, critical-materials-free solution to BTMS by employing a whole-systems approach. The focus of this initiative is to develop innovative battery energy-storage technologies with abundant materials applicable to PV energy generation, building energy-storage systems, EVs, and high-power charging systems. Solutions in the 1–10-MWh range will enable optimal integration of PV generation from a DC-DC connection, increase energy efficiency of buildings, eliminate potential grid impacts of high-power EV charging systems, and lower installation costs and costs to the consumer.

Many lessons learned from EV battery development may be applied to the BTMS program, but the requirements for BTMS systems are unique—carrying their own calendar-life, cycle-life, and cost challenges. For example, EV energy-storage systems need to meet very rigorous energy-density and volume requirements to meet consumer transportation needs. Despite that, current stationary storage systems use batteries designed for EVs due to high volumes that drive down the costs. This creates another market demand for EV batteries, further straining the EV battery supply chain and critical-material demand.

By considering BTMS electrochemical solutions optimized for these applications with less focus on energy density in mass and volume, the potential for novel battery solutions is very appealing. Furthermore, the BOP for a BTMS battery system, or the cost of everything minus the battery cells, is thought to be upwards of 60% of the total energy-storage system cost. In contrast, the EV's BOP costs make up roughly 30% of the total battery cost. Therefore, BTMS will also need to focus on reducing BOP cost through system optimization to realize desired cost targets.

Integration of battery storage with PV generation, energy-efficient buildings, charging stations, and the electric grid will enable new and innovative control strategies. The design parameters are needed to optimize the BTMS system for performance, reliability, resilience, safety, and cost.

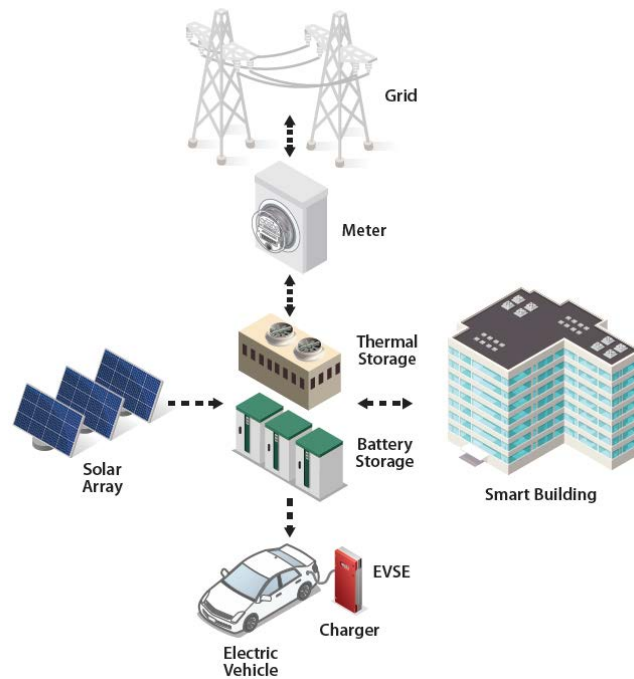


Figure 1. Overview of BTMS relevance.

Quarter 2 Milestone:

The Quarter 2 milestone for BTMS was: “Q2: Establish initial protocols and procedures for BTMS electrochemical energy cell evaluation that will enable feed back to the cost analysis task and the machine-learning physic-based model development tasks.” This milestone is reported on in the BTMS Testing and Protocols section, page 19, and is 100% completed.



BTMS Analysis: Electric Vehicle and Building Load Profiles

National Renewable Energy Lab (NREL)

Margaret Mann, Madeline Gilleran, Matt Mitchell, Darice Guittet, Eric Bonnema, Jason Woods, Chad Hunter, Monisha Shah, Andrew Meintz, Eric Wood

Summary

This Q2 Milestone report presents preliminary building and electric vehicle (EV) load profiles. The load profiles will be used as initial inputs for the EnStore multitool simulation platform to determine the optimal system designs and energy flows for thermal and electrochemical energy storage systems at sites with onsite photovoltaic (PV) generation. The report includes EV and building load profiles for the following three scenarios:

- Public DC fast chargers at a big-box retail + grocery store
- Level-2 chargers at a medium-size commercial office building
- Level-2 chargers at a low-rise multifamily residential apartment building.

This report first details the methods used to create both the EV and building profiles for each of these scenarios, and then presents the load profiles of the retail big box + grocery store, medium-size commercial office building, and low-rise multifamily residential apartment building, detailing the following:

1. EV station loads
2. Building loads
3. The combination of building + EV station loads.

Note that the load profiles demonstrated in this report are baseline EV and building profiles, which do not yet include the effects of solar PV electricity generation, stationary battery electrochemical storage (BESS), or thermal energy storage (TES). Baseline EV and building profiles will eventually exist for each of the building types scoped in the Annual Operating Plan: big-box retail + grocery store, three sizes (small, medium, and large) of commercial office buildings, fleet vehicle depot and operations facility, low-rise multifamily residential, and an EV charging station.

The static-load profiles generated in this report were shared with the larger Behind-the-Meter-Storage (BTMS) research team and used as a part of a separate calibration and modeling project funded by the Vehicle Technologies Office (VTO), focused on estimating battery lifetime. Additional results from that work will later be used in the EnStore model by the BTMS Analysis project in optimizing component sizes for the PV, BESS, and TES technologies. More information on this coordination can be found in the quarterly report submitted by Matt Shirk of Idaho National Laboratory (INL).

Background

The BTMS Analysis project is funded by the Buildings Technologies Office (BTO), VTO, and the Solar Energy Technologies Office (SETO) within the Department of Energy's (DOE's) Office of Energy Efficiency and Renewable Energy (EERE). The mission of EERE is to create and sustain American leadership in the transition to a global clean-energy economy. Its vision is a strong and prosperous America powered by clean, affordable, and secure energy. Increasing adoption of EVs, solar PV electricity generation, battery and thermal storage, and energy-efficient building technologies is expected to have a significant impact on energy use and domestic manufacturing. Each of these technologies can make contributions to the U.S. economy, but multiple

positive impacts can be gained by integrating them in ways that optimize cost and energy flows for varying energy demand and climate conditions across the country.

BTMS research is targeted at developing innovative energy storage technology specifically optimized for stationary applications that will enable fast charging of EVs, allow for enhanced grid-interactive energy-efficient buildings coupled with PV resources—all while minimizing grid impacts.

EV adoption is expected to grow significantly over the coming years and could have a significant—and potentially negative—effect on grid infrastructure due to large and irregular electricity demands. This is further complicated by the growth of variable-generation renewable energy technologies such as PV. In response to these changes, utilities are evaluating multiple options for managing dynamic loads, including time-of-use pricing and demand charges. Buildings and EV charging stations can leverage energy storage, including battery and thermal energy storage, coupled with onsite generation to stabilize the grid, manage energy costs, and provide resiliency and reliability for EV charging and building energy loads.

The key question in this project is the following: What are the optimal system designs and energy flows for thermal and electrochemical energy storage systems at sites with onsite PV generation and EV charging, and how do solutions vary with climate, building type, and utility rate structure?

Figure 1 shows a high-level schematic depicting the various behind-the-meter systems, including stationary battery, solar PV, electric-vehicle supply equipment (EVSE), and thermal energy storage.

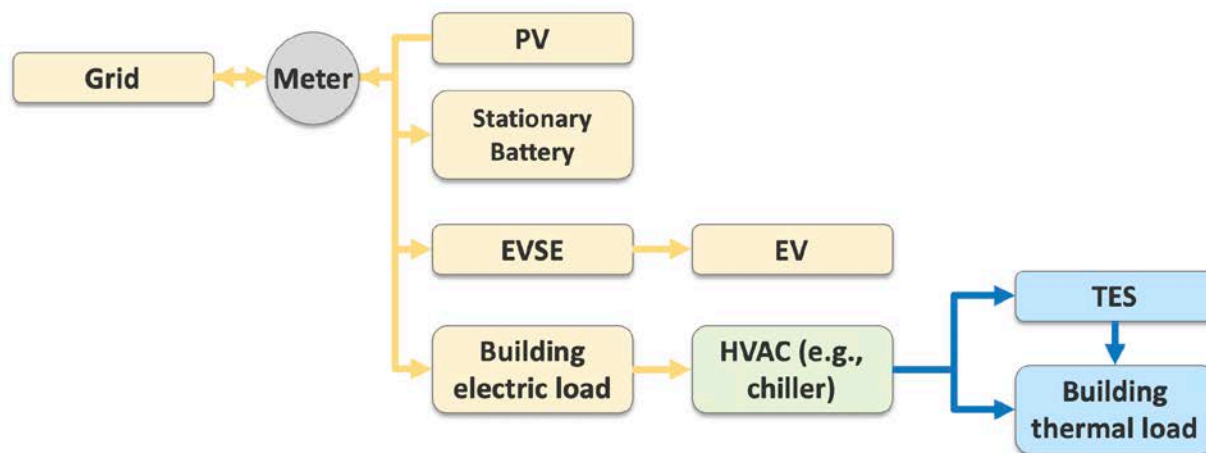


Figure 1. Schematic depicting the default combination of technologies for BTMS analysis.

The BTMS Analysis team is developing a multitool simulation platform called EnStore, short for Energy Storage. This platform will be able to capture performance characteristics and interactions between disparate technologies with high fidelity. *In researching existing tools used in this space, the team concluded that no one existing tool could complete the multisystem, detailed analysis required for this project; but rather, a combination of several existing tools would be necessary.* This project will leverage the following tools:

- REopt™ energy-system optimization tool (Cutler et al. 2017)
- System Advisor Model (SAM) (Blair et al. 2018)
- Electric Vehicle Infrastructure Projection Tool (EVI-Pro) (Wood et al. 2018)
- EnergyPlus™ building-simulation engine (DOE 2019a)

- OpenStudio® suite of supporting building-simulation applications (DOE 2019b)
- Utility Rate Database (URDB) (DOE 2019c)
- The DOE Prototype building-energy models (DOE 2019d)

Methodology for EV Load Profile Generation

EV load profiles for the BTMS analysis project will be simulated exogenously and input into the EnStore model at 10-year intervals (e.g., 2025, 2035, 2045) to assess how EV adoption, as well as changes in station design and station utilization, will affect usage and sizing of BTMS systems.

EV fleet makeup and percentage of total fleet estimations will be derived from RECHARGE analysis, including EVI-Pro simulations using Minnesota travel data. RECHARGE is a VTO-sponsored grid and infrastructure project investigating the benefits of smart charging and distribution impacts of EVs at scale. The project is analyzing adoption scenarios in Minneapolis and Atlanta, working with Xcel Energy and Georgia Power, respectively, to model additional EV load on real distribution feeders in these regions.

Results from EVI-Pro simulations that display the rate and length of each EV charging session are filtered and aggregated to create probability distribution functions (PDFs) for the arrival time, initial state of charge (SOC), and energy usage during each charge event for the various building types included in this analysis (e.g., home, workplace, and public charging). These PDFs will then be used as inputs to the EV-EnSite model, which generates year-long 1-minute EV load profiles. EV-EnSite is being developed as an extension of work performed by NREL and the University of Alabama, as described in Ucer et al. 2018. EV-EnSite will be integrated into the EnStore modeling framework for modeling varying EV demands across different building types and technology deployments.

In the EV-EnSite model, Monte Carlo simulations predict the charging load and queuing time at a station. During each EV-EnSite run, parameters such as time of arrival, energy demand, and initial SOC are stochastically regenerated from the input PDFs. During the Monte Carlo simulations, vehicles arrive at the corresponding stations, wait in the queue if there is not any available port to plug into, are plugged in if a port is available, and are then charged according to their charge acceptance curves. They depart the port after their energy demand is met, and a new vehicle from the queue is plugged into an available port (Ucer et al. 2018).

Inputs to the EV-EnSite include the following:

- Station design, including port capacity and number of plugs
 - Station utilization, including frequency of charging events per plug at each station
 - Types of plug-in hybrid or battery EVs arriving at the station, including battery capacity and battery chemistry
 - Three probability distribution functions, including:
 - Arrival time, or the time of day when vehicles arrive at the station
 - Initial SOC, or the SOC of the vehicles when they arrive at the station
 - Energy charged in event, or the energy, measured in kWh, taken from the grid in each session, which is a PDF that is tied to initial SOC (i.e., if a vehicle arrives with a low SOC, then there is a greater chance it will charge for a longer duration)
-

Methodology for Building Load-Profile Generation

EnergyPlus, a whole-building energy-simulation engine, along with OpenStudio, a suite of complementary tools that can expand EnergyPlus capabilities, are being used as a part of the EnStore analysis. These tools will be used in both the Pre-Processing Stage and the Exploration Stage, seen in Fig. 2.

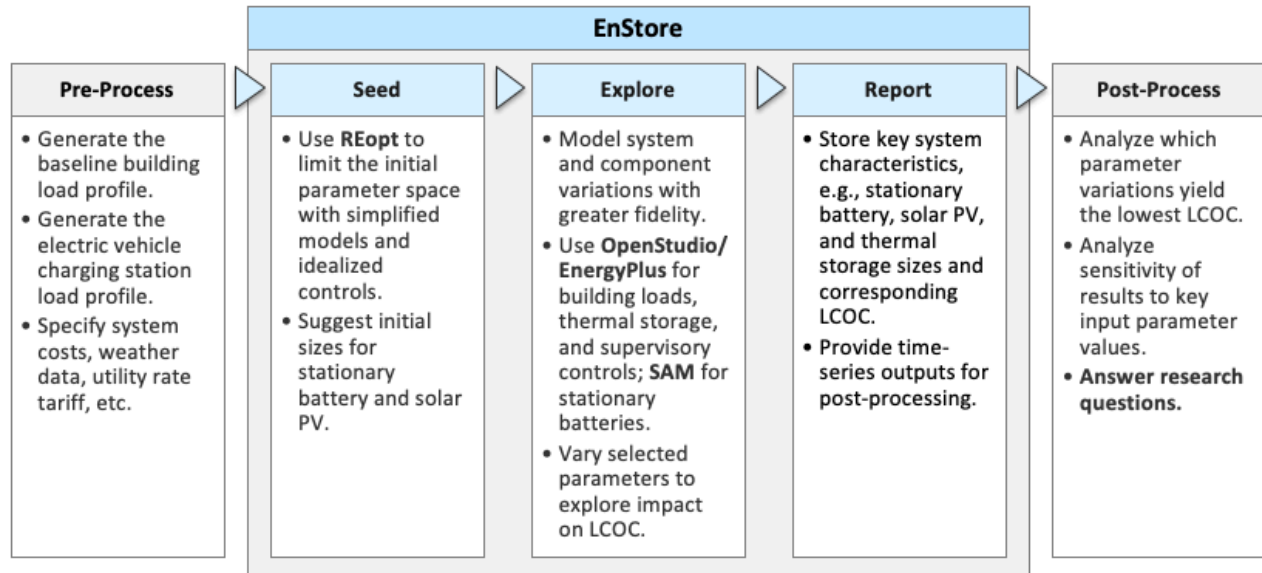


Figure 2. Major stages of the multitool workflow.

In the Pre-Processing Stage, OpenStudio is used to generate a static 15-minute interval timeseries load profile as an input to REopt, to seed the system with potentially optimal sizes. In the Exploration Stage, EnergyPlus performs annual simulations to capture the complex interactions of (among others) EV loads, building loads, and onsite generation (PV) and storage (TES and BESS).

For each EnStore run, a baseline building model—one that has no solar PV, stationary battery, or thermal energy storage—will be simulated. A different baseline building model will be created for each of the building types included in this project (big-box retail + grocery store, commercial office building, fleet vehicle depot and operations facility, multifamily residential, and an EV charging station). In EnergyPlus/OpenStudio, measures will be applied to these baseline models to add solar PV, stationary battery, and TES of various sizes to assess what is optimal from a financial perspective.

The building load profiles seen in this report were generated from running EnergyPlus models in Tucson, Arizona, which has high air-conditioning (A/C) demands in the summer as well as high solar-energy potential.

Big-Box Retail + Grocery Store: EV and Building Loads

The first BTMS case to be analyzed is a big-box retail grocery store (e.g., Walmart Supercenter, SuperTarget, Kroger Marketplace) with public EV fast-charging stations delivering 350 kW of power per plug. It is assumed that, at least to begin the analysis, these EV fast-charging stations will be used by grocery store customers and not by heavy-duty delivery trucks.

Big-Box Retail + Grocery Store EV Load Profiles

Since the number of EV ports at a big-box retail + grocery store location will likely increase over time as EV demand increases, it was initially assumed that the number of ports in 2025 will be two. In 2035, however, there may be four, and in 2045, there may be six. These particular station design assumptions were made

because current EVGo fast-charging stations often have two ports, and a typical current gas station at a big-box retail grocery store has 20 ports. However, even if EVs did penetrate 100% of the market, 20 ports may be unreasonable because EV owners can refuel at home or work, whereas all internal-combustion-engine vehicles must refuel at gas stations.

The probability distribution functions for arrival time, initial SOC, and energy consumed during a charging event are derived from EVI-Pro results using California travel survey data created from prior work completed by NREL and the California Energy Commission; however, in the future, these PDFs will be generated from work for the RECHARGE project, with travel data used from Minnesota.

Because the frequency of events, or number of events per day per plug, has high variation among sites, the following three cases will be analyzed:

- A high utilization case (16 events per day)
- An average utilization case (8 events per day)
- A low utilization case (2 events per day).

Based on initial EVGo data analyses, which are detailed in the following section, there is no great variation in frequency of events from weekday to weekend. So, no weekend or weekday variation in events per plug per day was assumed for this building type (Muratori, 2019).

Example EV Load Profiles: Two Monte Carlo Simulations

To generate the two day-long load profiles in Fig. 3 for a public EV fast-charge station, inputs included six total plugs at the station and eight events per plug per day. The two plots are slightly different due to the inherent Monte Carlo stochasticity, because time of arrival, energy demand, and initial SOC for each EV charging event is randomly regenerated from the input PDFs.

Although the number of plugs is lower for this public fast-charge station than that for office and multifamily residential, the total station peak power levels are significantly higher. This is not only because the frequency of events is higher, but also, because the power delivered to the vehicle in DC fast charging (compared to L1 or L2 charging) is much greater.

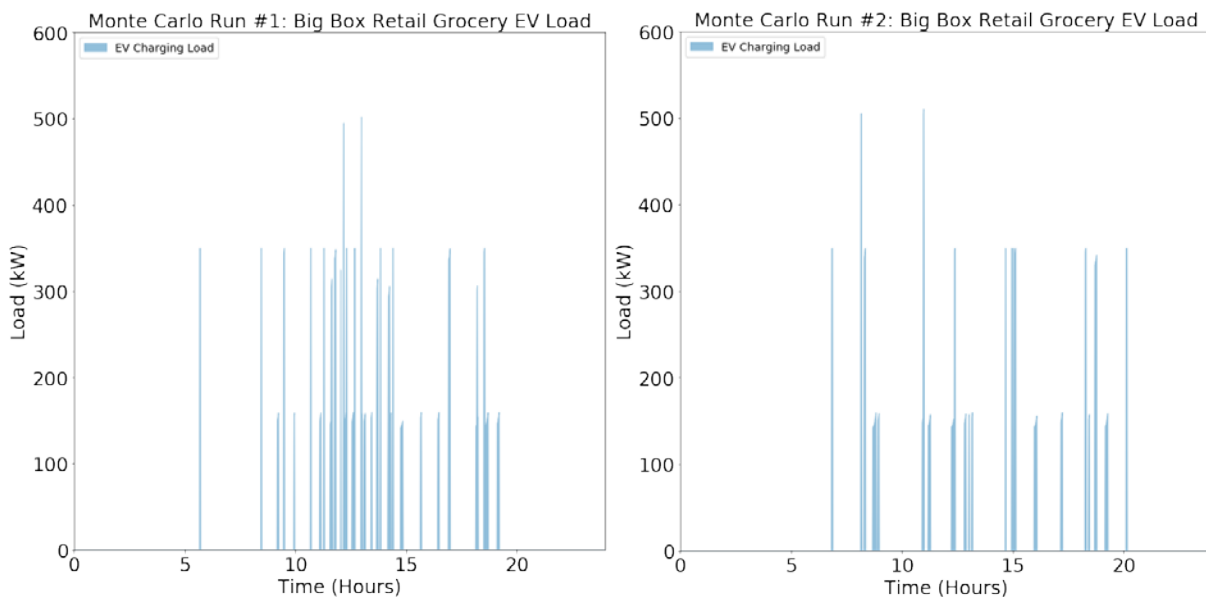


Figure 3. Schematic depicting two Monte Carlo simulations to generate two day load profiles for a public station.

Load Profile Variance: Varying Station Design and Station Utilization

Figure 4 and Figure 5 show day-long EV load profile outputs, and varying number of ports and number of events per day per port at a station. It is likely that the port count at an EV charging station will increase as demand increases and that frequency of charging events per port will also increase over time. However, it may be possible that stations will initially be oversized (i.e., ports initially underutilized) to accommodate the likely increasing frequency of charge events with growing EV adoption.

Six-Port Station

Below are load profiles with varying utilization for a six-port station. Low utilization is two events per plug per day; medium utilization is eight events per plug per day; high utilization is sixteen events per plug per day.

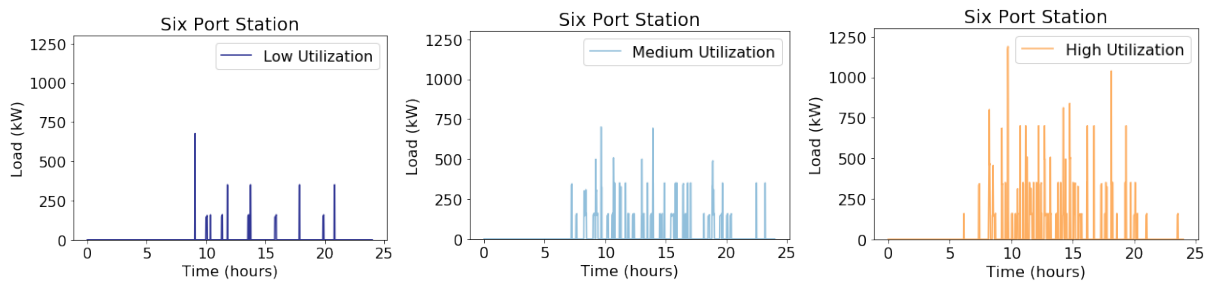


Figure 4. Schematic depicting how station utilization affects the load profile for a six-port station.

Two-Port Station

These are load profiles with varying utilization for a two-port station. Low utilization is two events per plug per day; medium utilization is eight events per plug per day; high utilization is sixteen events per plug per day.

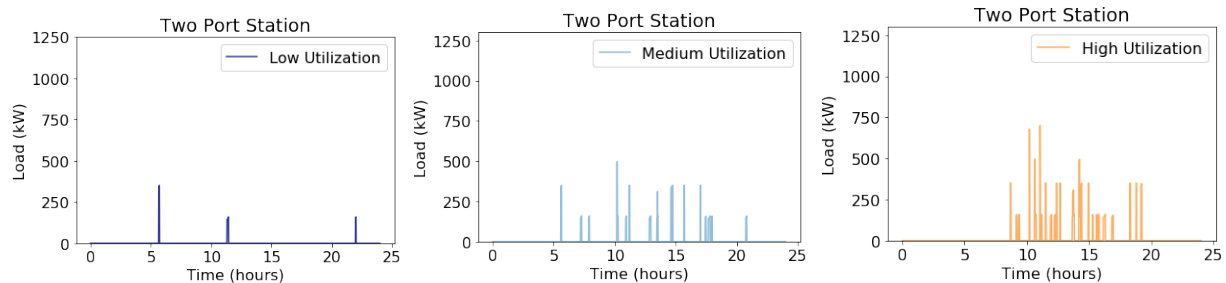


Figure 5. Schematic depicting how station utilization affects the load profile for a two-port station.

Analysis to Determine Station Utilization: Events per Plug per Day

EVGo data from 2017 (Table 1) was used in assessing what could be reasonable assumptions for the number of events per day per charger input to the EV-EnSite model to generate the EV load profiles (Muratori, 2019). The EVGo stations analyzed are 50-kW fast-charging stations spread throughout the United States—in San Francisco, San Diego, Los Angeles, Washington D.C., and Boston. As seen in Table 1, many stations have two chargers per site.

Table 1. EVGo High Variance in Average Charging Events per Day per Port for Different Properties

Property	Market	Min	Avg	Max	# Chargers	Avg Events per Day per Charger
Site 1	SF	0	64	99	4	16
Site 2	SD	1	24	48	2	12
Site 3	SF	0	17	38	2	9
Site 4	SD	0	16	37	2	8
Site 5	LA	0	16	39	2	8
Site 6	LA	0	12	26	2	6
Site 7	DC	0	12	51	2	6
Site 8	SF	0	11	23	2	5
Site 9	SD	0	10	25	2	5
Site 10	SF	2	17	34	4	4
Site 11	LA	0	8	27	2	4
Site 12	DC	0	3	20	2	2
Site 13	BOS	0	4	22	2	2
Site 14	BOS	0	2	18	2	1
Site 15	BOS	0	2	17	2	1

This analysis helped inform the high utilization case for the BTMS analysis of 16 events per day per plug. This utilization level is reached at the “busiest” EVGo station, or Site 1, where the average events per day per charger is 16. The low utilization case for the BTMS analysis was chosen to be two events per day per plug, which is seen at some of the sites in Table 1.

Retail Big-Box Grocery Store Building Load Profiles

The EnergyPlus model of big-box retail + grocery store was generated as part of a separate project for a retail big-box grocery store located in Centennial, Colorado. This model was calibrated with sub-metered data from the store. For this analysis, we simulated the building in Tucson, Arizona. A full-year profile can be seen in Fig. 6(a), and a day-long timeseries can be seen in Fig. 6(b), with both EV and building profiles in minute resolution. Note that the load peaks in the middle of the year due to high summer A/C and grocery refrigeration demands.

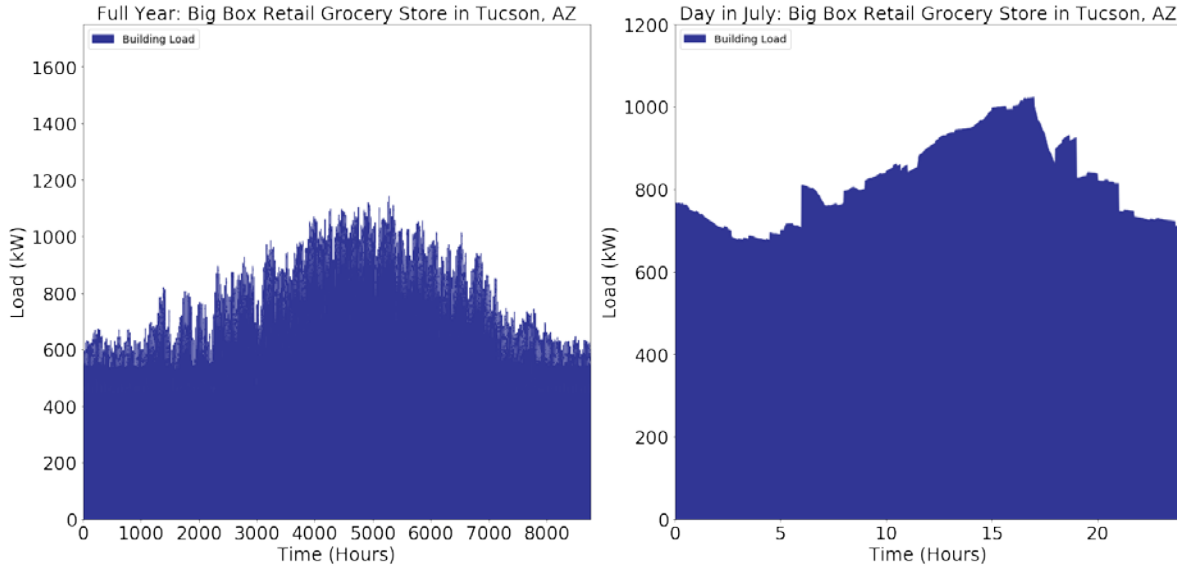


Figure 6. (a) Year-long and (b) day-long power timeseries profiles of retail big-box grocery store.

Big-Box Retail + Grocery Store EV and Building Loads: Combined

To compare magnitudes between the EV load profiles and building load profiles, the EV and building load profiles were combined. Figure 7(a) and Figure 7(b) show that, for this scenario, the EV load profile is fairly significant, with similar magnitude compared to that of the electric-building load profile.

To obtain a year 2030 EV load profile for the retail big-box grocery store, a two-port, 16-event per day per port station was assumed. In 2030, it is likely that two ports would be in place at a station, rather than four or six ports, because many EVGo stations have two ports. However, utilization in 2030 will likely be higher than that seen today at a public EV charging station. Therefore, 16 events per port per day was selected, because that was seen earlier in Table 1 in the busiest EVGo station.

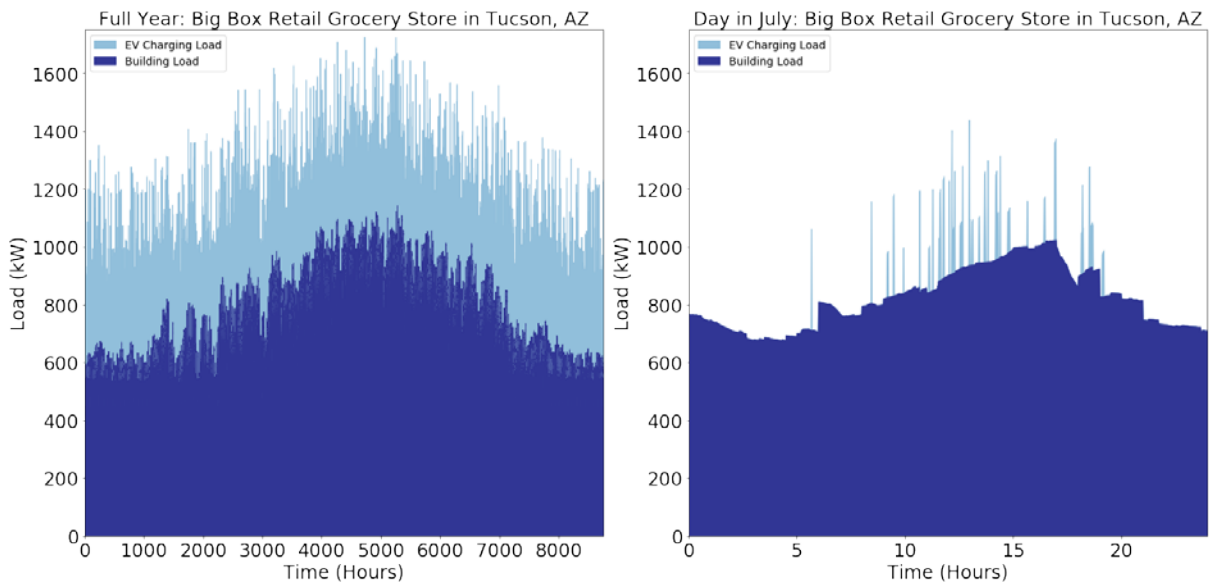


Figure 7. (a) Year-long and (b) day-long power timeseries profiles of retail big-box grocery store and EV station.

Medium-Size Commercial Office: EV and Building Loads

A medium-size office building will be modeled using the DOE Prototype for medium commercial office building, with Level-2 chargers delivering 6.6 kW of power per plug.

Medium Commercial Office EV Load Profiles

It is assumed that the charging level will be L2 at 6.6 kW for this scenario because people are generally at an office for long periods of time; therefore, an expensive fast-charging infrastructure is not necessary. It is also assumed that number of events per day per plug will vary between one and two, because office workers will likely not desire to leave their office space to move their car throughout the day. There is likely variation of utilization between weekday and weekend for this case, with zero to one event per day per port on the weekends when many people do not come into work.

Example EV Load Profiles: Two Monte Carlo Simulations

To generate these two day-long load profiles (Fig. 8) for an office building, the inputs regarding station design and station utilization are the same, with 20 total plugs at the L2 (6.6 kW) station and one charge event per plug per day.

The two plots are slightly different due to the inherent variation teased out in Monte Carlo simulations, because time of arrival, energy demand, and initial SOC for each EV charging event is stochastically regenerated from the input PDFs. Note that for this office scenario, due to the arrival time PDF input, most charging events occur at the beginning of the day when EV owners are typically at work.

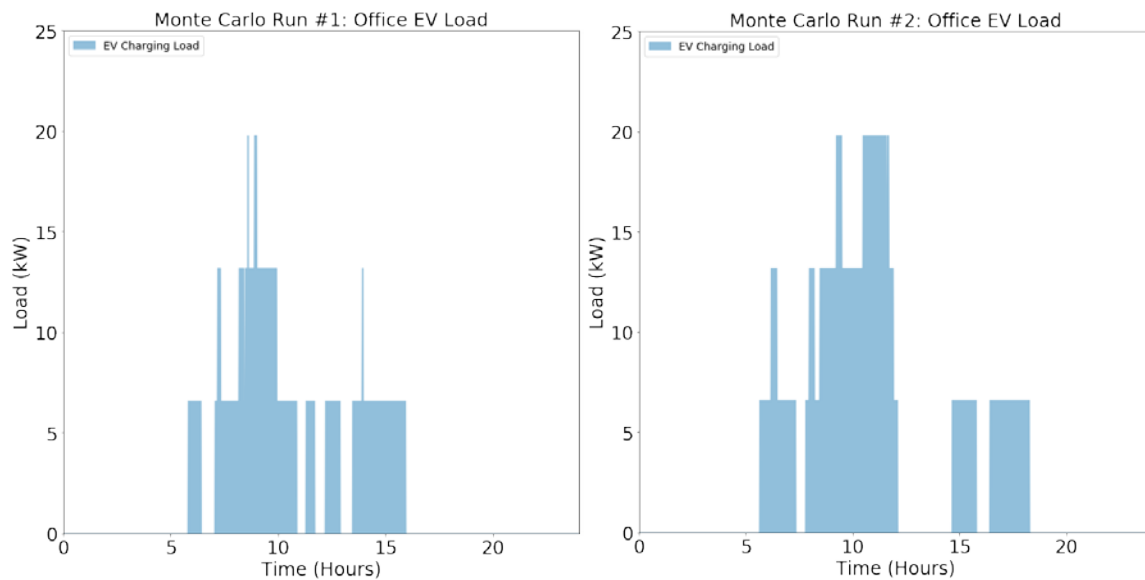


Figure 8. Schematic depicting two Monte Carlo simulations to generate EV profiles for an office station.

Medium Commercial Office Building Load Profiles

The DOE medium office prototype model (run in Tucson, Arizona) was used to represent a typical medium-sized office building. A full-year load profile can be seen in Fig. 9(a), and a day-long timeseries can be seen in Fig. 9(b). Note that the DOE Prototype model has a spike at the beginning of each day due to the electric reheat terminals cycling on as the building thermostats return from nighttime setback.

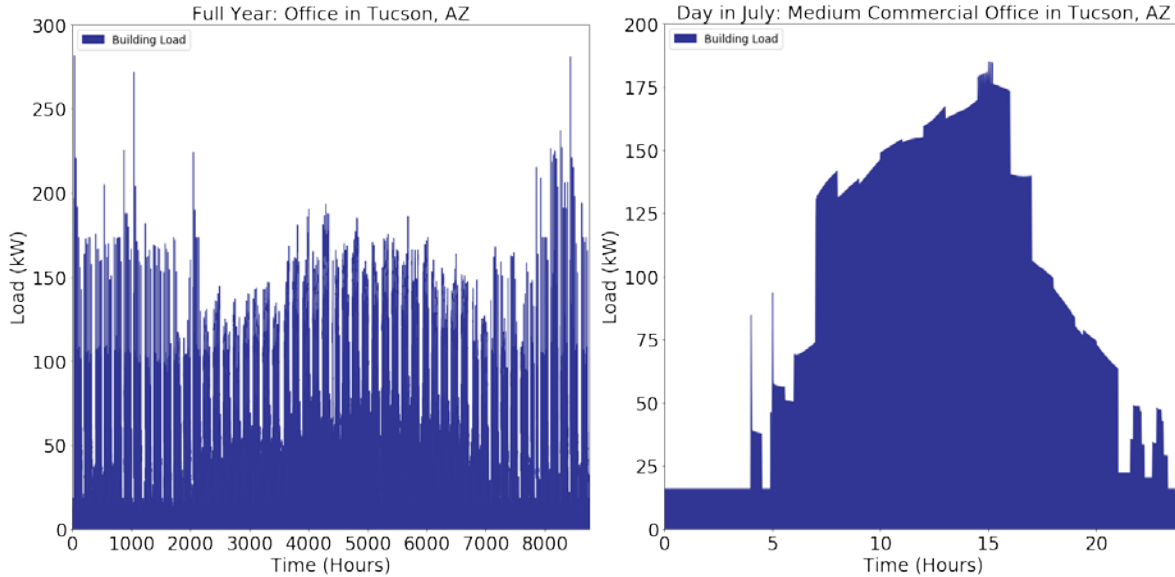


Figure 9. (a) Year-long and (b) day-long power timeseries profiles a medium-size commercial office.

Medium Commercial Office EV and Building Loads: Combined

To compare magnitudes between the EV load profiles and building load profiles, the EV and building load profiles were combined. As shown in Fig. 10(a) and Fig. 10(b), for this scenario, the average daily energy consumed by EVs is fairly insignificant compared to that of the building.

To obtain the EV load profile for the medium office building, the 2030 Electric Power Research Institute (EPRI) High Battery Electric Vehicle (BEV) Scenario was used, as is also used in the RECHARGE project. This case predicts 13.2% BEV penetration.

The DOE Prototype medium office building assumes 268 occupants. Based on the ratio of 0.6 parking spaces per occupant—a general rule of thumb used to determine the number of spots at the NREL parking garage [Myers, Lissa]—this results in about 161 parking spots for the medium office building. Assuming everyone parking at work with a BEV can and will charge at the office on a regular basis, then 13.2% of all parking spots, or 22 ports, may be an appropriate estimation for the size of the station. To generate the EV load profile, it was also assumed that there would be one charge event per day per plug.

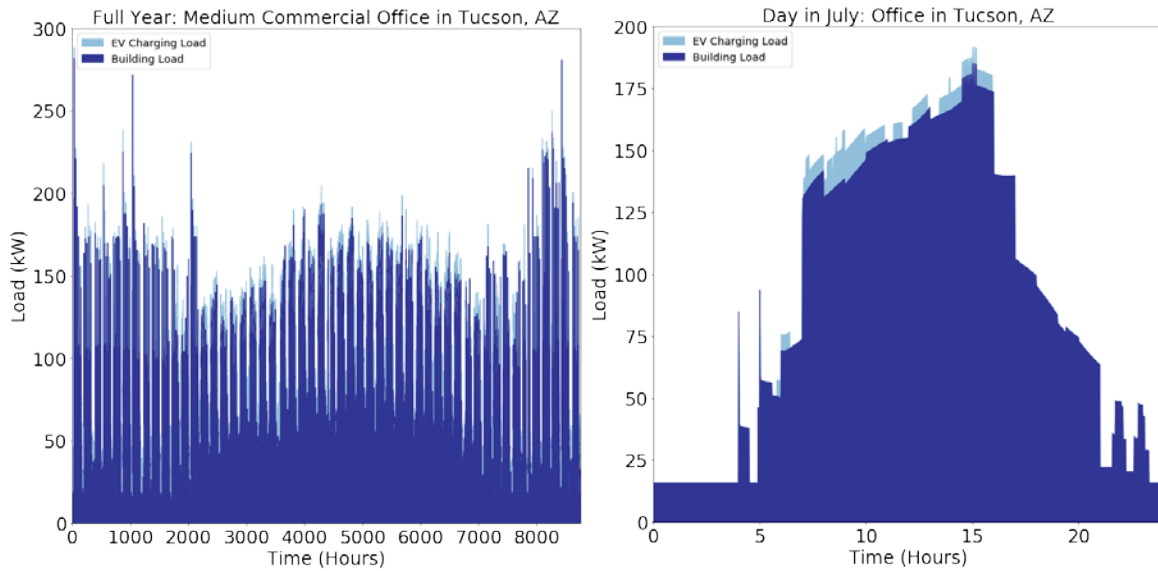


Figure 10. (a) Year-long and (b) day-long power timeseries profiles of a medium commercial office and EV station.

Multifamily Residential: EV and Building Loads

The multifamily residential load profile will be generated using the DOE Prototype for the mid-rise apartment building, with Level-2 chargers delivering 6.6 kW of power per plug. The high-rise apartment DOE Prototype building could have also been selected for this use case, but the mid-rise apartment captures a larger portion of the multifamily residential population—because high-rise apartments are usually found in downtown urban areas, whereas mid-rise apartments can be found in both urban and suburban areas.

Multifamily Residential Apartment EV Load Profiles

For this building type, it is assumed that the charging level will be L2 at 6.6 kW because people generally dwell at their homes for long periods, usually during the evening; therefore, expensive fast-charging infrastructure is not necessary. It is also assumed that number of events per day per plug will vary between one and two, because those living in an apartment will likely not be inclined to move their car in the middle of the night to allow for another vehicle to charge. It is uncertain whether variation of utilization between weekday and weekend occurs for this case, but it likely will not, because instead of working during the day, people are often running errands and doing activities on the weekend and will still charge primarily at night.

Example EV Load Profiles: Two Monte Carlo Simulations

To generate the two day-long load profiles in Fig. 11 for a multifamily residential building, the inputs regarding station design and station utilization levels are the same as that of the medium commercial office building—with 20 total plugs at the L2 (6.6 kW) station and one event per plug per day.

These are the same station design and station utilization inputs as for an office; that is, the number of plugs at the station and frequency of charging events per plug are identical. However, the load profiles are quite different because more charging events occur in the evening when EV owners are home.

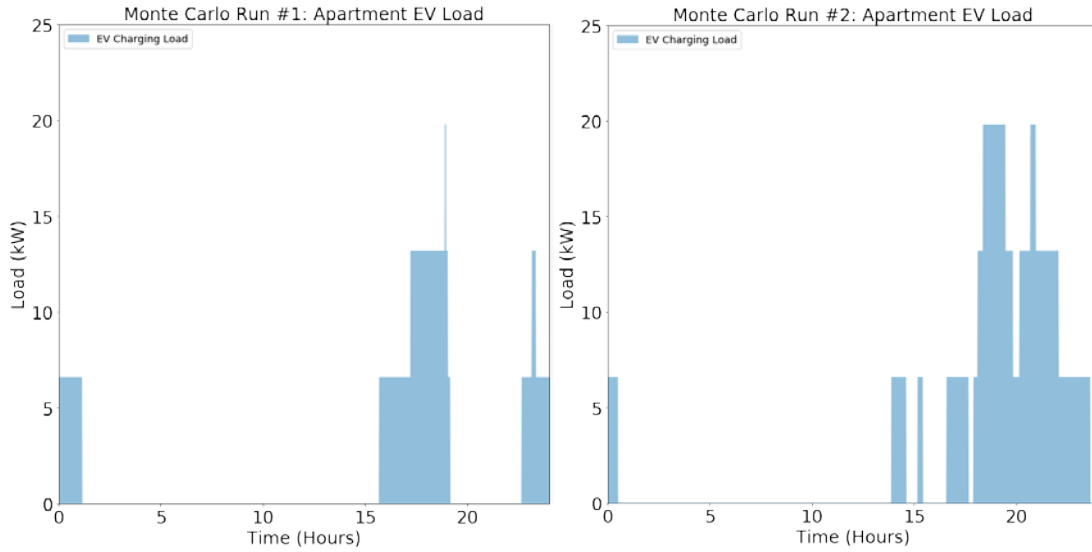


Figure 11. Schematic depicting two Monte Carlo simulations for a multifamily residential building.

Multifamily Residential Apartment Building Load Profiles

The DOE mid-rise apartment prototype model (run in Tucson, Arizona) was used to represent a typical multifamily residential building. A full-year load profile can be seen in Fig. 12(a), and a day-long timeseries can be seen in Fig. 12(b).

As seen in Fig. 12(a), the load is very high at the beginning of the year, likely due to convergence anomalies in the simulation trying to reach steady state. Seen in Fig. 12(b), the rapidly cycling load throughout the day is due to the 23 in-unit electric water heaters. This creates a highly variant power profile that may be problematic given the needs of this project to have a relatively accurate estimate of demand at minute intervals. So, the BTMS team plans on changing the electric water heaters in the existing DOE Prototype building model to natural gas heaters, which may actually be more realistic because that is the current primary heating fuel. The BTMS analysis team will take measures to remove irregularities from any existing models to generate a robust minute-interval power load profile.



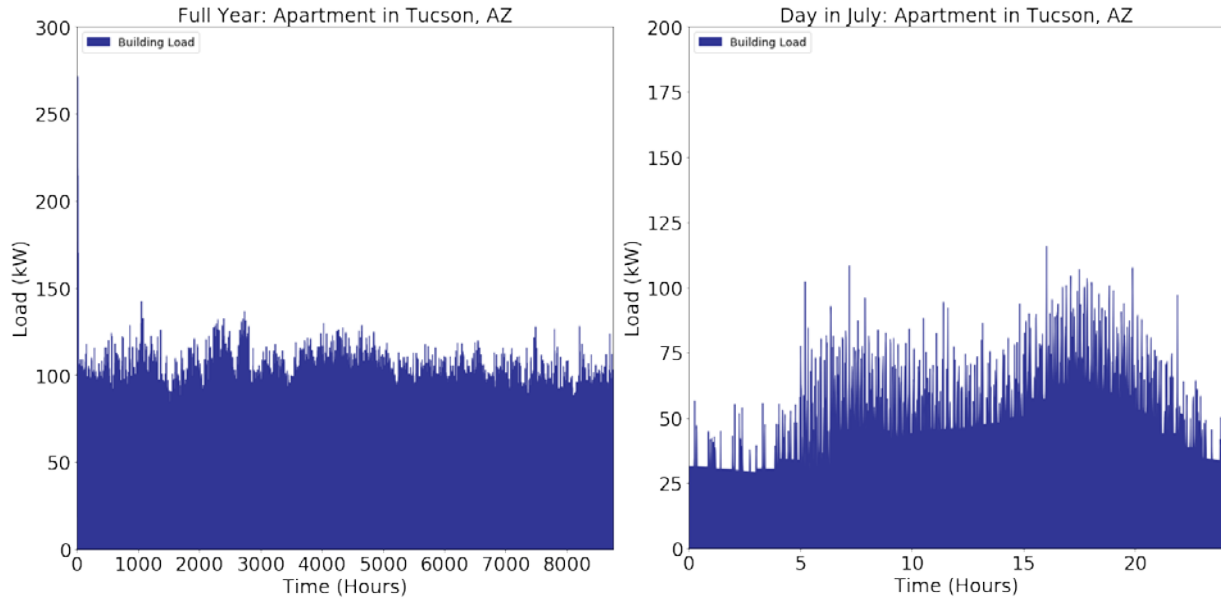


Figure 12. (a) Year-long and (b) day-long power timeseries profiles a multifamily residential building.

Multifamily Residential Apartment EV and Building Loads: Combined

To compare magnitudes between the EV load profiles and building load profiles, the EV and building load profiles were combined. As shown in Fig. 13(a) and Fig. 13(b), for this scenario, the average daily energy consumed by EVs is fairly insignificant compared to that of the building.

To obtain the EV load profile for the multifamily residential building, the 2030 EPRI BEV Scenario was again used, predicting 13.2% BEV penetration. Assuming the mid-rise apartment has 67 occupants, and using the parking rule of thumb, there are likely 39 parking spots at this site. Assuming 13.2% of those parking spots have EV charging options, six ports exist at this building type.

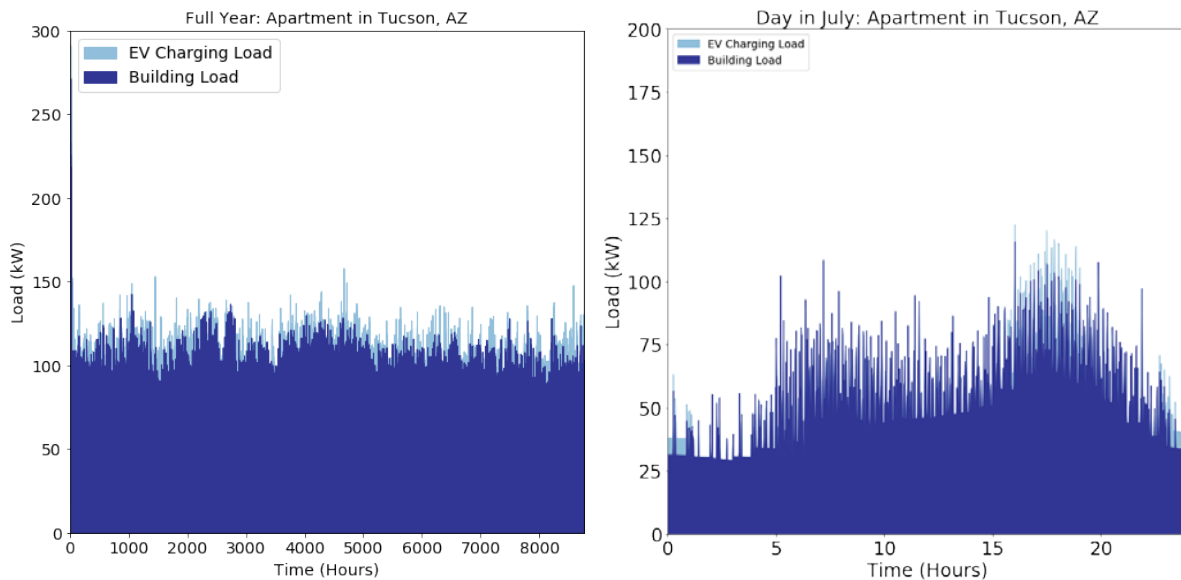


Figure 13. (a) Year-long and (b) day-long power timeseries profiles a multi-family residential building and EV station.

Conclusion

This quarterly report presents initial building and EV load profiles that will be used as inputs for the EnStore framework. These profiles detail initial progress that has been made to obtain EnStore inputs, as improvements needed to make the BTMS results as robust as possible. Comparison of building and EV loads for one week in April for the big-box retail + grocery, medium office, and mid-rise apartment can be seen in Fig. 14. Note that the big-box retail + grocery building and EV station uses much more energy than the office or apartment building because the big-box + retail store is very large and has high loads (e.g., HVAC, refrigeration, lighting).

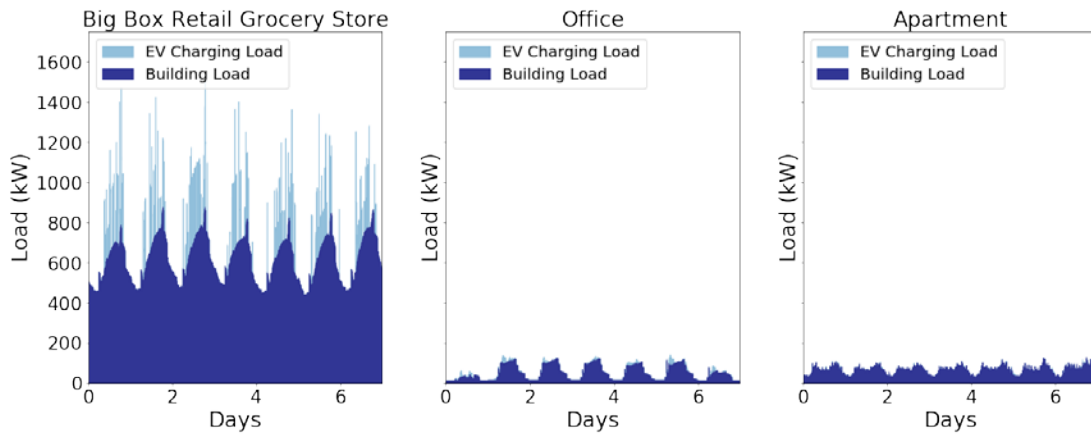


Figure 14. Comparison of retail big-box grocery store, office, and apartment EV and building load profiles.

As seen in Fig. 15, when comparing just the office and apartment buildings loads for one week in April, the office loads are dramatically lower on the weekends (the first and last day of the week seen). Note also that the EV loads for the office complex are higher than that for the apartment complex because the office has higher occupancy, and therefore, more EV ports.

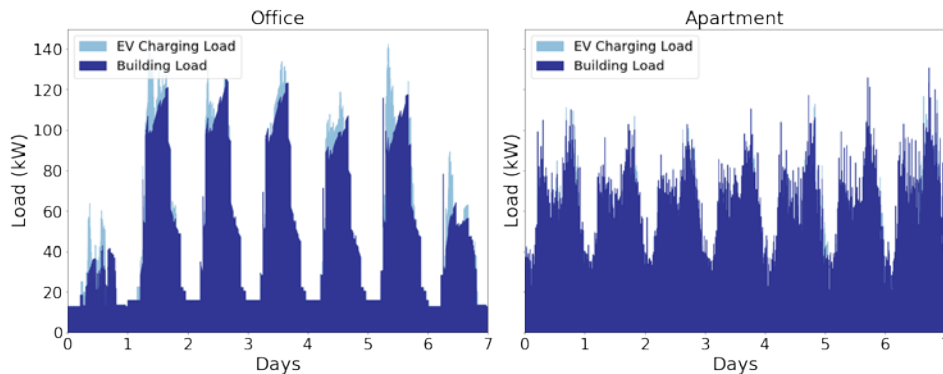


Figure 15. Comparison of office and apartment EV and building load profiles.

Figure 16 compares the EV loads for one day for each of the three building types: retail big-box grocery store, medium commercial office, and multifamily residential. The big-box retail + grocery store, with DC fast chargers at 350 kW, has much shorter and higher-power charging events than the medium office and mid-rise apartment.

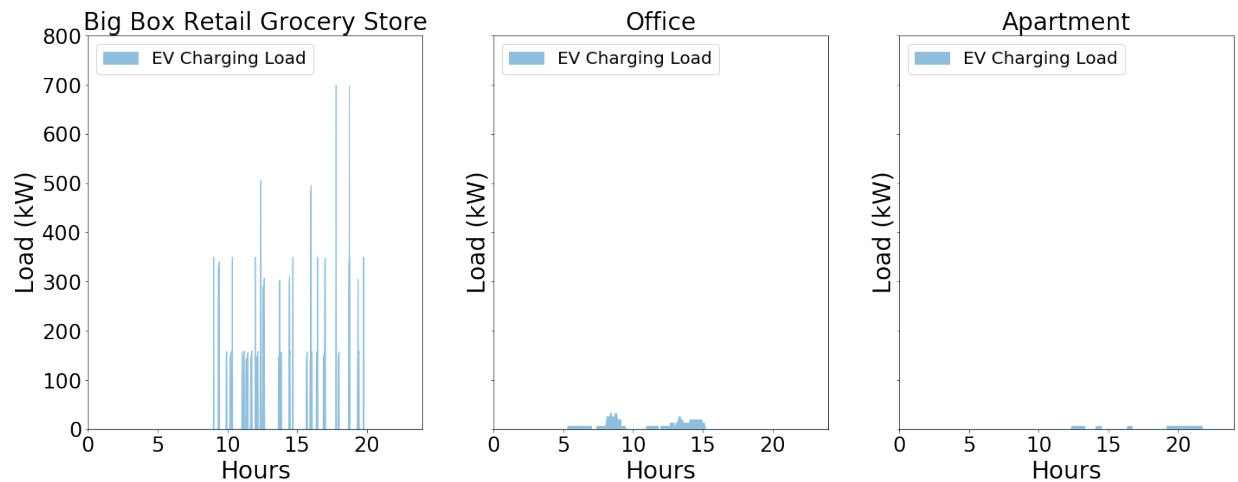


Figure 16. Comparison of retail big-box grocery store, office, and apartment EV load profiles.

Seen in Fig. 17, when comparing just the office and apartment EV station loads for one day, the charging events for the office often occur in the morning and throughout the day while many are at work. However, the charging events for the apartment complex occur largely in the evening and throughout the night because this is when the majority of people are at home.

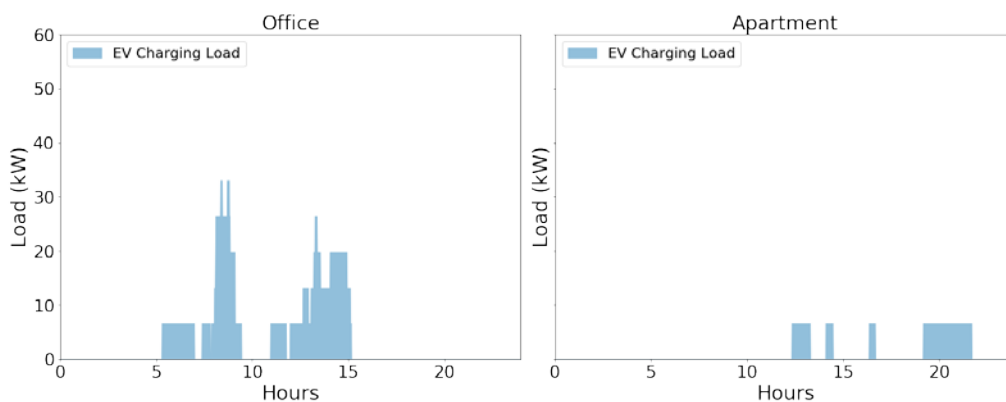


Figure 17. Comparison of office and apartment EV load profiles.

Next Steps

The next steps for this project include the following:

- Refining building models and EV load profiles
- Testing initial EnStore runs on the high-performance NREL supercomputer
- Completing end-to-end model testing.

Regarding refining the building models, the DOE Prototype medium office and multifamily residential buildings will be improved for more accuracy on an energy-demand (kW) basis because the DOE Prototype models were initially created to be accurate only on a monthly-energy (kWh) usage standpoint. This includes evaluating the assumptions of the model and comparing the models to existing field data, when possible. The algorithms used to control and dispatch the building HVAC equipment also will be evaluated to ensure realistic control of equipment, such as by controlling for zone temperature setpoints with appropriate dead

bands, rather than load-based controls. Utility rate structures will also play a role in determining how the building HVAC equipment is dispatched, which will also help refine the building models for more realistic energy-demand profiles.

Regarding refining the EV load profiles, implementing the EVI-Pro outputs from the RECHARGE project as well as general assumptions made from RECHARGE will be incorporated into the EV load profiles. Initial load profiles for the other building and EV load profiles, including vehicle fleet depot and EV charging station, will also be explored.

To complete end-to-end model testing, the EnStore multitool simulation platform will soon be able to use REopt to seed solar PV and stationary battery sizes and create deviation from that preliminary seed to run EnergyPlus and SAM simulations. EnergyPlus will be able to call the PySAM battery model at each timestep of the simulation. EnergyPlus output load profiles (net electric loads from the grid and net electric loads put back to the grid) correlated with their respective battery, PV, and TES sizes will be used to compute net present costs (NPC), levelized cost of charging (LCOC), and other financial metrics, with system designs selected to minimize costs for the system owner. These simulations will be able to be run locally or on the NREL high-performance supercomputer to enable the millions of simulations necessary to explore and answer the questions of the BTMS analysis project.

References

- Blair, N., N. DiOrio, J. Freeman, P. Gilman, S. Janzou, T. Neises, M. Wagner. 2018. *System Advisor Model (SAM) General Description (Version 2017.9.5)*. Golden, CO: National Renewable Energy Laboratory (NREL). NREL/TP-6A20-70414. <https://www.nrel.gov/docs/fy18osti/70414.pdf>.
- Cutler, D., D. Olis, E. Elgqvist, X. Li, N. Laws, N. DiOrio, A. Walker, K. Anderson. 2017. *REopt: A Platform for Energy System Integration and Optimization*. Golden, CO: National Renewable Energy Laboratory (NREL). NREL Technical Report No. NREL/TP-7A40-70022. <https://www.nrel.gov/docs/fy17osti/70022.pdf>.
- Dey, Satadru, Ying Shi, Kandler Smith, Andrew M. Colclasure, and Xuemin Li. (March 2020). “From Battery Cell to Electrodes: Real-Time Estimation of Charge and Health of Individual Battery Electrodes.” *IEEE Transactions on Industrial Electronics* 67, no. 3: 2167–75. <https://doi.org/10.1109/TIE.2019.2907514>.
- DOE (U.S. Department of Energy). 2019a. “EnergyPlus.” <https://www.energyplus.net>.
- DOE (U.S. Department of Energy). 2019b. “OpenStudio.” <https://www.openstudio.net>.
- DOE (U.S. Department of Energy). 2019c. “Utility Rate Database.” https://openei.org/wiki/Utility_Rate_Database.
- DOE (U.S. Department of Energy). 2019d. “Commercial Prototype Building Models.” https://www.energycodes.gov/development/commercial/prototype_models
- Muratori, Matteo “Technology solutions to mitigate electricity cost for electric vehicle DC fast charging,” *Applied Energy*, vol. 242, pp. 415–423, May 2019, doi: 10.1016/j.apenergy.2019.03.061.
- Myers, Lissa (personal communication, January 29, 2020) discusses the employee count to parking ratio rule of thumb for NREL. Sustainable Transportation and Climate Change Resilience Manager at the National Renewable Energy Lab (NREL).
- Short, W., D. J. Packey, T. Holt. 1995. “Manual for the Economic Evaluation of Energy Efficiency and Renewable Energy Technologies.” *NREL Technical Report*. <https://www.nrel.gov/docs/legosti/old/5173.pdf>
-

Ucer, E., M. Kisacikoglu, F. Erden, A. Meintz, C. Rames. 2018. "Development of a DC Fast Charging Station Model for use with EV Infrastructure Projection Tool." *2018 IEEE Transportation Electrification Conference and Expo (ITEC)*: 904-909. <https://doi.org/10.1109/ITEC.2018.8450158>.

Wood, E., C. Rames, M. Muratori. 2018. "New EVSE Analytical Tools/Models: Electric Vehicle Infrastructure Projection Tool (EVI-Pro)." Golden, CO: National Renewable Energy Laboratory (NREL). NREL Presentation No. NREL/PR-5400-70831. <https://www.nrel.gov/docs/fy18osti/70831.pdf>.

BTMS Testing and Protocols

Contributors: INL, SNL, NREL

Background

Cycle-life-testing profiles were developed to test against BTMS-supported Extremely Fast-Charging (XFC) scenarios. The information produced from the testing can be used to scale the device-level results up to the system level for various station configurations, in conjunction with the cost-modeling task. The cycle-life profile is presented in this report. Additionally, life testing continues for a few selected commercial lithium-ion cell types to probe their performance relative to early BTMS life goals. The status of this ongoing testing is presented and discussed, along with planned testing activities.

Results

Cycle-Life Protocol Development

Overview and Methodology

The cycling routine developed is a method of cycling an energy storage device at the design threshold of an energy storage system (ESS)-augmented XFC station designed to minimize utility power demand. Two XFC station design metrics define the maximum use-case cycle for the ESS device: 1) XFC station continuous-use time, which translates to BTMS battery continuous discharge time between full charges, and 2) XFC station usage time that is designed to be accommodated for in a 24-hour period; this translates directly to the maximum time period that must be supported by the BTMS battery in a 24-hour period. From these station design parameters, we can define two metrics used in the cycling procedure: 1) discharge time target, defined simply as the continuous XFC station continuous-use time design requirement, expressed in hours, and 2) charge time target, defined by the amount of time in a 24-hour period that the BTMS system is not discharging, divided by the number of BTMS battery cycles needed in that 24-hour period to meet the total daily discharge time requirement; with all times expressed in hours, this reduces to the equation below:

$$\text{Charge Time Target} = \frac{[\text{Discharge Time Target}] * (24 - [\text{total daily discharge time}])}{[\text{total daily discharge time}]}$$

If a nominal XFC duration is defined, the continuous and total-daily discharge times can be expressed in number of back-to-back and daily XFC events supported, respectively. In Table 1, a 10-minute XFC event was chosen to illustrate the number of events that could be supported at the design threshold for three different scenarios. These are not finalized design cases, but rather, early estimations of practical station designs.

Table 1. Relationships between station design parameters and resulting cell cycling parameters based on usage at design threshold.

XFC Duration (Minutes)		Peak-Day Station Design Parameters					Max-Usage Results					Lifetime Implications		
10		XFC Events per Day	Back-to-Back XFC Events	Total Discharge Hours per Day	Max BTMS Battery Cycles per Day	Discharge Time per Cycle	Max Charge Time per Cycle	BTMS Share of XFC Input Power (rough)	Minimum Years to 10,000 Cycles	Years to 10,000 Cycles if Avg usage = 0.5 Design Peak	Maximum Number of Cycles in 20 Years	Number of Cycles in 20 years if Avg usage = 0.5 Design Peak		
24	6	4	4	1.0	5.0	0.83	6.8	13.7	29,200	14,600				
24	12	4	2	2.0	10.0	0.83	13.7	27.4	14,600	7,300				
36	18	6	2	3.0	9.0	0.75	13.7	27.4	14,600	7,300				

The size of the system that would be built would then depend on the total input power to the XFC station that needs to be supported by the BTMS battery. The share of total input power delivered to the XFC station by the BTMS system can be approximated, as shown below, given that the energy used to recharge the BTMS system is nearly evenly spread over the charge window. In this approximation, system efficiency is not included.

$$BTMS \text{ Share of XFC Input Power} \sim 1 - \frac{\text{Discharge Time Target}}{\text{Discharge Time Target} + \text{Charge Time Target}}$$

A better approximation of the share of power delivered by the BTMS system—a measure of demand reduction capability—would be determined by also factoring in the inefficiency of the BTMS charge process, and the 15-minute peak power used in the charge procedure; but these will not be known until characterization testing is conducted.

It is important to consider that the cycling routine presented is not intended to represent an actual usage scenario, where the arrival timing of vehicles, XFC event durations, and XFC power levels would be expected to vary significantly, affecting depth of cycling, discharge power profile, and rest periods. Rather, this tests the cycle-life capability of a device against usage at the design threshold. The next section outlines the terms used in the cycling procedure that immediately follows.

Glossary of Testing Terms

Beginning-of-Life (BOL) – The point in time, prior to cycle or calendar aging, when the device is initially characterized.

Charge Time Target ($T_{\text{chg,target}}$) [h] – The period over which a BTMS battery must be able to be recharged to its maximum operating state of charge (SOC), following a discharge of length Discharge Time Target at the Target Discharge Power.

Discharge Power Target ($P_{\text{dis,target}}$) [W] – The discharge power used, at the device level, for cycling.

Discharge Time Target ($T_{\text{dis,target}}$) [h] – The minimum period over which a BTMS battery must be able to supply its discharge power, from its maximum operating SOC.

Discharge Voltage Limit ($V_{\text{limit,dis}}$) [V] – The minimum cell voltage, that upon reaching the discharge must be terminated.

End-of-Life (EOL) – The point in time when the device can no longer discharge at its discharge power target, $P_{\text{dis,target}}$, for the duration of Discharge Time, T_{dis} .

Energy Fade Allowance [%] – The amount of fade in Usable Energy allowed before a device is considered end-of-life. This allowance is used to calculate the time and usable energy margin at BOL, needed to allow the device to fade to an EOL condition while meeting the constant discharge time and power requirements throughout life.

Maximum Operating SOC ($\text{SOC}_{\text{max,op}}$) [%] – The state of charge to which the battery will be charged every cycle. This may be less than the cell’s absolute maximum SOC.

Peak Charge Power ($P_{\text{chg,peak}}$) [W] – The highest average power over a rolling 15-minute window observed when following the charge protocol.

Usable Energy (UE) [Wh] – The measured energy discharged from the device—from $\text{SOC}_{\text{max,op}}$ to $V_{\text{limit,dis}}$ —at the fixed discharge power, P_{dis} .

Cycling and Calendar Protocols

The following steps must be followed at BOL to determine the values to be used throughout life testing for each scenario against which a device will be tested, and for each device type tested.

- A. Set the following constants, based on an XFC station design, such as those illustrated in Table 1, which will be fixed throughout the duration of life testing:
 - a. Discharge Time Target, $T_{dis,target}$
 - b. Charge Time Target, $T_{chg,target}$
- B. Set the following constants, to be fixed throughout the duration of life testing, based on the specifications of the device to be cycled:
 - a. Max Operating SOC, $SOC_{max,op}$
 - b. Discharge Voltage Limit, $V_{limit,dis}$
 - c. Energy Fade Allowance (%)
 - d. Cycling Temperature(s)
- C. Determine Discharge Power
 - a. Find the device power that discharges the Usable Energy (UE) of the device in the time period $\frac{T_{dis,target}}{1 - \text{Energy Fade Allowance}}$. For example, a 1-hour discharge time target and an energy fade allowance of 20% yields $\frac{1h}{0.8} = 1.25 h$. Iteration of discharge power will be necessary to determine this value, although a starting point can be based on constant-current capacity ratings and nominal voltages. Results from this test, once completed, will yield BOL UE.
- D. Set Charge Procedure
 - a. The charging procedure for a normal cycle must return the cell to its Maximum Operating SOC ($SOC_{max,op}$) within the Charge Time Target ($T_{chg,target}$). The charge should be chosen such that the peak charge power is as close to the average charge power as possible. Any rests, post-discharge or post-charge, that are necessary for stable cycling should be included in the charge period. The procedure may also leave a time margin to allow for degradation in device power acceptance.

The cycling protocol steps are described below.

1. Charge the cell to $SOC_{max,op}$ using the charge procedure above.
2. Rest until the end of $T_{chg,target}$, if necessary.
3. Discharge the cell, constant power, at $P_{dis,target}$, for the time $T_{dis,target}$. If $V_{limit,dis}$ is reached, the device has reached EOL condition.
4. Repeat steps 1–3, until 99 discharges (as detailed in step 3 above) have been performed; then perform the following subroutine:
 - a. Rest for 1 hour at the end of the 99th discharge.
 - b. Charge the cell to $SOC_{max,op}$, using the same charge procedure as in the above cycling procedure.
 - c. Rest for 1 hour after the end of the charge period.
 - d. On the 25th discharge, discharge the cell, constant power, at $P_{dis,target}$, until $V_{limit,dis}$ is reached.
 - e. Rest for 1 hour, then resume steps 1–4 above, except that the charge following the 100th cycle reference test should not be time-limited like the typical charge used in cycling.
 - a. Discharge the cell, constant power, at $P_{dis,target}$, until $V_{limit,dis}$ is reached.
 - b. Rest for 1 hour, then resume steps 1–3 above, except that the charge following this reference test should not be time-limited like the typical charge used in cycling.

Discussion

The XFC station parameters that affect discharge and charge times that are set in step A are likely to evolve as scenario development matures. A given device type may be tested against multiple XFC station scenarios, each having its unique pair of Discharge and Charge Time Targets. The device-specific parameters that are set in

step B should be based on the available specifications for each device type, and the choice of these is intended to maximize lifetime throughput for the device. Max Operating SOC and Energy Fade Allowance can be chosen strategically to cycle the device in a particular SOC window—either to maximize throughput, or to decrease device charge and discharge rates by oversizing the system, or a combination of both. The primary cycling temperature chosen should be based on an ideal, or reasonable, operating temperature for the device, although additional elevated temperatures may be chosen to give additional information on the life impacts of minimal thermal conditioning. A primary cycling temperature would be 30 °C for many devices, and additional temperatures might be 40 °C and 50 °C.

Once the parameters that define the test cycle for a device are set, the device will be cycled to remove a fixed amount of energy, accomplished by discharging at a constant power for a fixed period. Every 100th cycle will include a deep discharge, measuring the total time period over which the discharge power target is available, and the amount of usable energy available. This measurement allows us to track the degradation in usable energy capacity as the cell ages. The Usable Energy discharged is a measure of both cell capacity and impedance, because both will affect the capacity at which the discharge cutoff voltage is reached. The device state-of-health can be monitored from these reference deep discharges based on the degree to which the measured Usable Energy approaches the EOL limit determined by the Energy Fade Allowance. End-of-Life is reached when a normal discharge cycle cannot produce the Discharge Power Target over the Discharge Time Target.

The resulting life capability data can be applied back into the cost analysis task, and these baseline aging procedures will be supplemented by accelerated aging and analysis methods that are being developed jointly with the machine-learning and physics-based model development tasks. Specific data to be provided to the cost optimization and analysis task, for each device tested, include:

- Scenario upon which the cycling results are based, and all cycling parameters used
 - Discharge Power Target used for cycling
 - Discharge Time Target used for cycling
 - Peak Charge Power
- Unit cost of device
- Device mass and envelope volume
- Number of cycles and energy throughput to EOL
- Test temperature(s).

These device-level results can be scaled up to system sizes designed to support any XFC power level, and lifetime costs, including the need to replace cells or modules, will be determined.

Additionally, maximum and minimum device voltage limits used in cycling will be provided to the power electronics design task. This information would help in determining the DC voltage operating range of operation of power-conversion devices, which can affect those costs.

Ongoing Testing

INL

One graphite/NMC622 EV cell continued to cycle shallowly in the middle 50% SOC range, and it shows slightly extended life when using a significantly smaller capacity compared to its deeply cycled twin. The difference and the incremental increase in cycling data collected since the last report are shown in Fig 1. below.

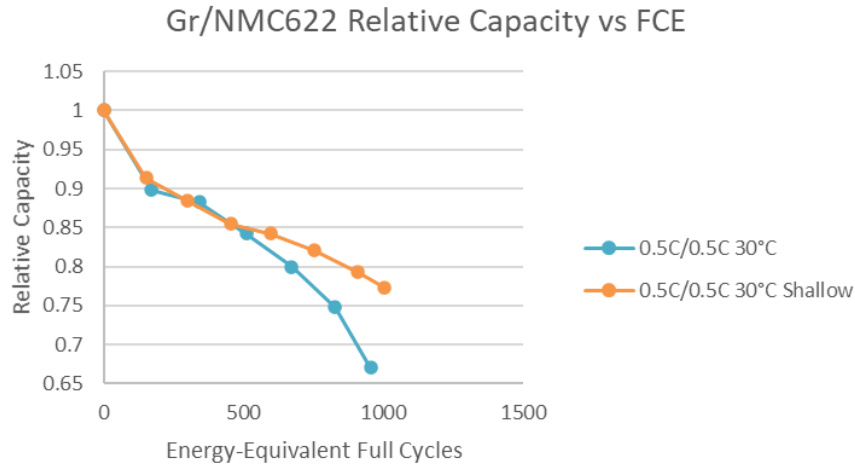


Figure 1. Graphite/NMC622 0.5C/05C full-depth and shallow cycle life capacity retention at 30°C.

LTO/NMC cells optimized for long cycle life, but having a significantly lower specific energy, continue cycle and calendar aging using accelerating conditions with very little capacity loss observed, as shown in Fig. 2. Manufacturer literature on these cells suggests 80% capacity retention after 60,000 1C/1C cycles at 30 °C. Visual inspection of these cells shows no excessive gassing to date.

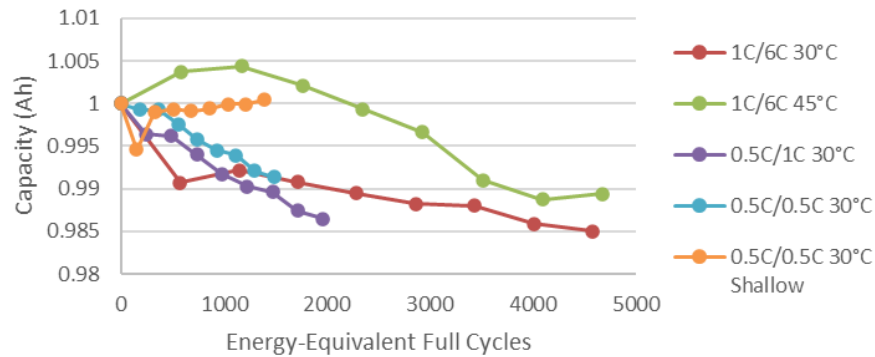


Figure 2. LTO/NMC cycle life capacity loss for a variety of rates and temperatures.

SNL Testing

Two different cell constructions are currently being investigated for the LFP/Graphite system. These cells have undergone continuous cycling until the target of 1000 cycles was reached. The effects of this cycling on the capacity fade of the cells can be observed in Fig. 3.

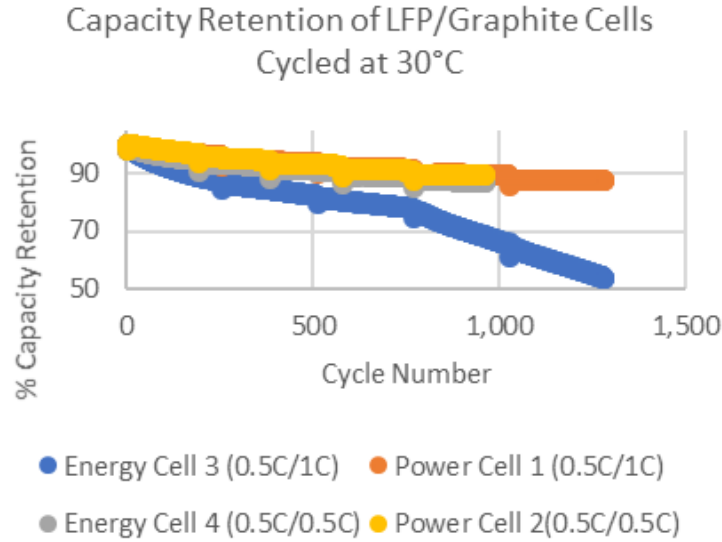


Figure 3. LFP/graphite cycling results.

Results show that, on average, the power cells have lost ~10% while the energy cells have lost close to ~50% in the worst case. It is difficult to say that the ~50% loss in the energy cell is representative without additional cells to provide statistics. If we target a 50% capacity retained at end of life after 10,000 cycles, then the capacity fade rate would need to be 0.005% capacity fade/cycle. These data suggest that the capacity fade rate of this chemistry in this form factor exceeds the desired decay rate by factors of ~2–5, indicating that these cells should not meet our lifetime targets. Differences in the state-of-health testing of these cells can also be observed as demonstrated in Fig. 4.

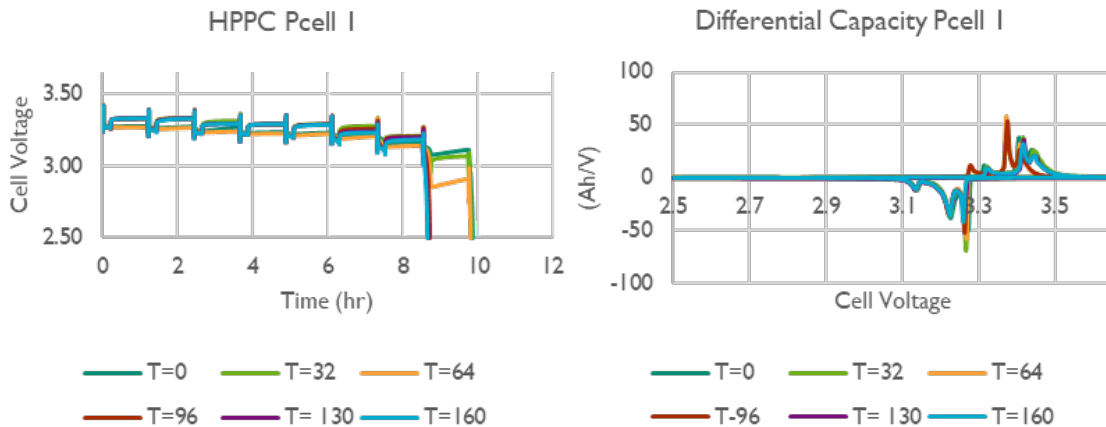


Figure 4. Power cell 1 state-of-health testing of LFP/graphite cells.

HPPC results show that as the cell continues to cycle, it loses its ability to deliver power at low states of charge. Understanding this phenomenon will be critical for predicting end-of-life behavior of these cells. The differential capacity results suggest that the loss of performance is most likely attributed to changes in the

graphite anode, which is a known problem—graphite is known to degrade from extensive cycling. As work continues on electrolyte and electrode work, these hurdles may be overcome.

Upcoming Testing

Toshiba LTO/LMO cells have been delivered, and initial check-in receipt has been performed at INL. ZAF Ni Zn cells were planned for shipment on March 15th; however, their delivery has been delayed until INL's lab resumes normal operation. The LTO/LMO is advertised to have very long cycle life, and the nickel zinc cells are touted as low cost and extremely recyclable, although cycle life is not expected to approach the BTMS goal without changeout. Both types of cells are critical-material-free and will be used as some of the first devices to shake down the BTMS cycle-life protocol.

Summary

Aging continues on commercial cells that began early in the program, not meeting the critical-material-free BTMS goal. New critical-material-free commercial cells are planned for testing and evaluation to serve as a benchmark for thick-electrode, critical-material-free cells being designed specifically for BTMS applications and for use in testing the newly developed cycling protocol.

Power Electronics for Behind-the-Meter Storage

National Renewable Energy Laboratory
Ahmed Mohamed, Ram Kotecha, Andrew Meintz

Background

The power electronics effort for BTMS has been tasked with evaluating methods to reduce the balance-of-plant (BOP) cost associated BOP components for a stationary battery system. The technology target for the entire BTMS system ranges from \$295/kWh to \$235/kWh, for a C/1 or C/4 charging station target. The BOP, including the power conversion, is roughly two-thirds of the system cost. From a power perspective, the BOP equates to \$0.195/W and \$0.540/W between the two station designs (C/4 and C/1). In the FY19 analysis of current-state stationary energy storage systems considering at least a 1-MW system with a 13.8-kV connection, the BOP costs ranged from \$0.40 to \$1.01/W. An investigation of the various power-conversion topologies (AC-coupled, DC-coupled, and multiple bus DC-coupled) will be investigated to determine strategies for the entire site to optimize the design of the BOP. The task objectives for investigation of the primary power-conversion optimization are as follows:

- Explore different configurations for integrating ~ 2-MW DC fast-charging (DCFC) loads, ~ 2-MW PV generation, and ~2-MW energy storage system (ESS) with the power grid:
 - Conventional common AC bus configuration
 - New common DC bus configuration
 - Modular-based multiple DC bus
- Estimates efficiency vs. load curve for the power electronic conversion stages for:
 - DC fast chargers (350-kW ports)
 - PV generation
 - Grid ESS
 - Grid interface (e.g., transformer, and AC/DC converter)
- Integrate the conversion efficiency data with EnStore platform for system cost analysis.

Results

The team has defined the possible configuration for a site integrated with ~ 2-MW DCFC loads, ~2-MW PV generation, and ~2-MW ESS with the power grid. Three different configurations are considered:

A. Conventional common AC bus configuration (Fig. 1):

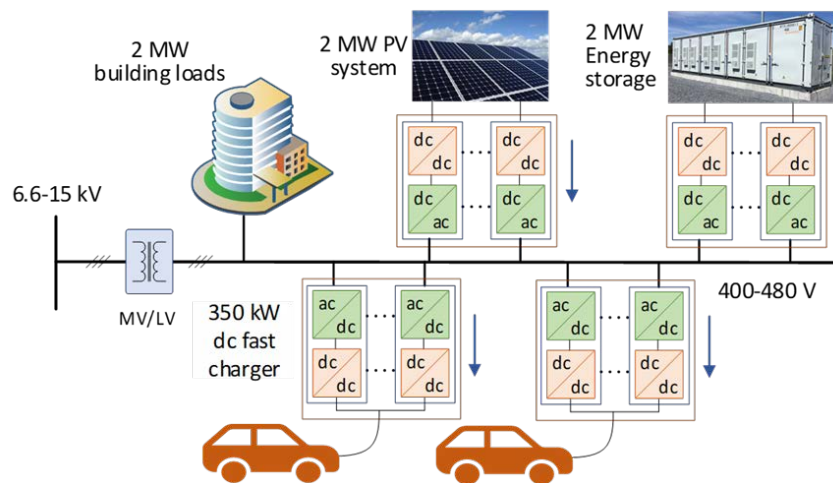


Figure 1. Conventional common AC bus integration.

B. Common DC bus configuration (Fig. 2):

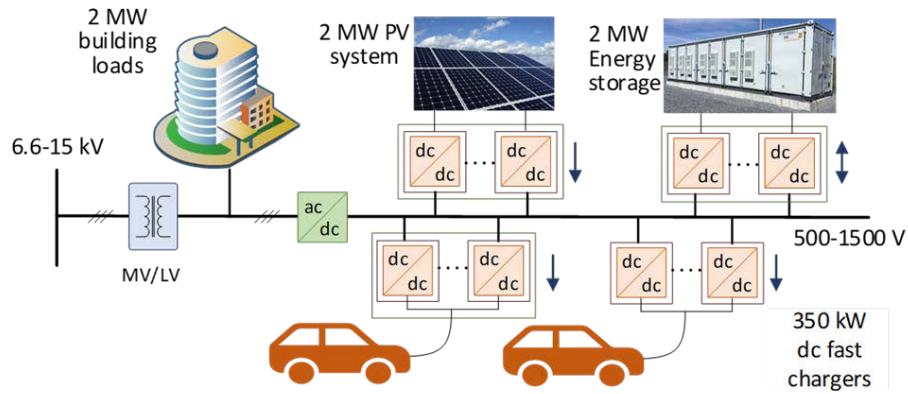


Figure 2. Common DC bus microgrid integration.

C. Modular-based multiple DC bus configuration (Fig. 3):

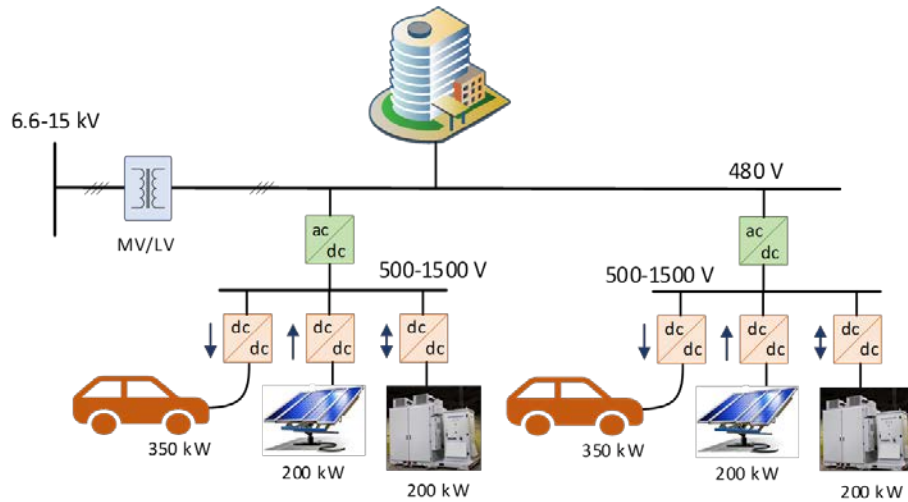


Figure 3. Modular-based multiple DC bus microgrid integration.

The team is working to develop the load-efficiency curve data for the conventional common AC bus configuration, shown in Fig. 1. In this configuration, all generation and load is coupled to the grid through a common low-voltage (480 V) AC bus. A medium-voltage/low-voltage transformer is used to bring the voltage down. PV, ESS, and DCFC are connected to the AC bus through two conversion stages: AC/DC and DC/DC. A modular concept is considered to size the 2-MW system level.

For DCFC, the commercial 160–350-kW ABB Terra HP DCFC (Fig. 4) is considered. Typically, vehicles do not request the same power at the same time, so the current configuration considers sharing three 170-kW units to provide 350-kW and 160-kW charging capability from the same charge post, as indicated in Fig. 4. Therefore, a 2-MW charging station will include four of these configurations (12×170 kW).

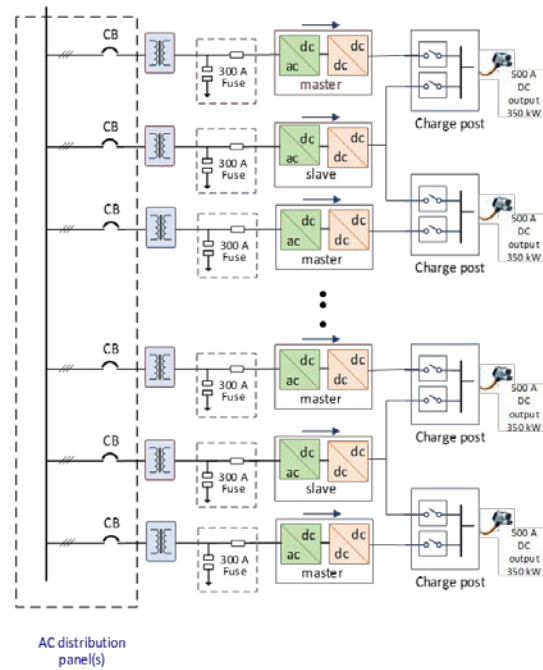


Figure 4. Schematic diagram of conventional ~2-MW DCFCs system.

The load-efficiency curves for the energy conversion of a 350-kW DCFC are evaluated including isolation transformer and power electronics. Figure 5 shows the variation of the energy-conversion efficiency as the loading conditions change. It presents different profiles at different average operating temperatures.

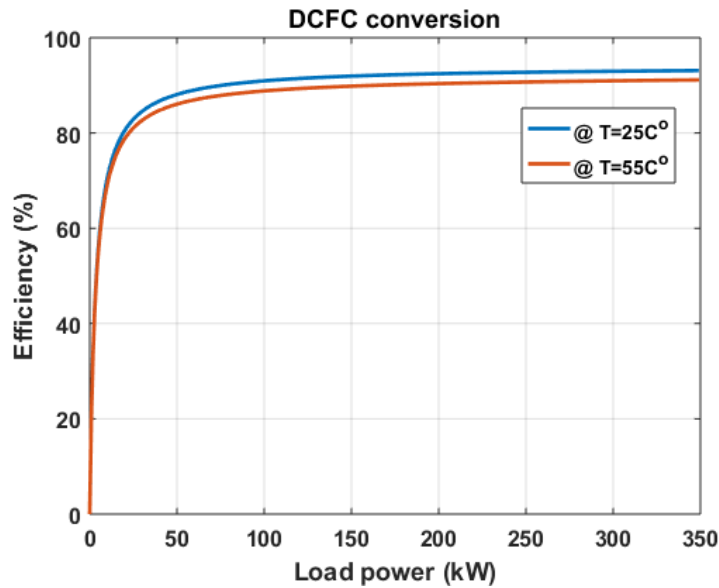


Figure 5. Estimated load-efficiency curves of 350-kW DCFC conversion system.

For PV generation, the commercial SMA Sunny Central 550CP PV Inverter (Fig. 6) is considered. For a 2-MW PV generation, four of these configurations (4×550 kVA) will be installed.

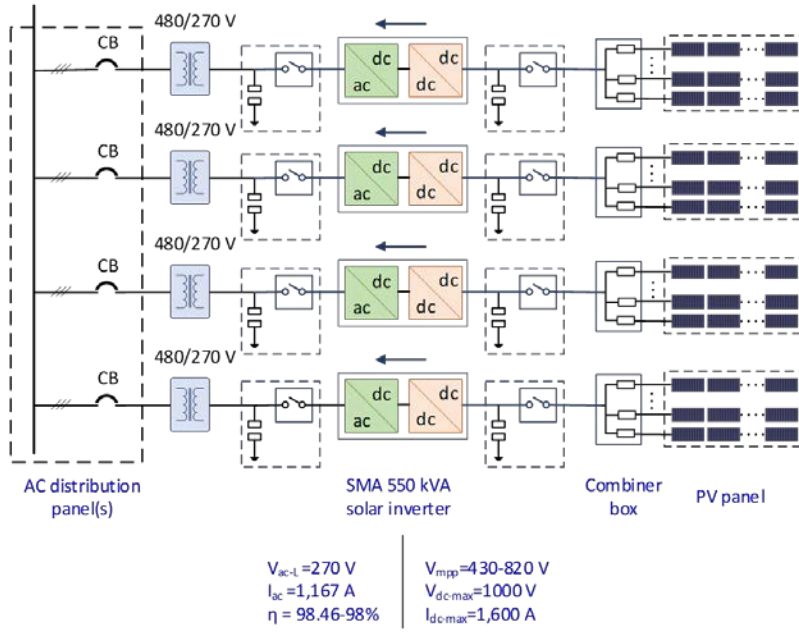


Figure 6. Schematic diagram of conventional ~2-MW PV system.

The load-efficiency curves for the energy conversion of a 550-kW PV generation are evaluated including isolation transformer and power electronics. Figure 7 shows the variation of the energy-conversion efficiency as the loading conditions change along with the impact of average operating temperatures.

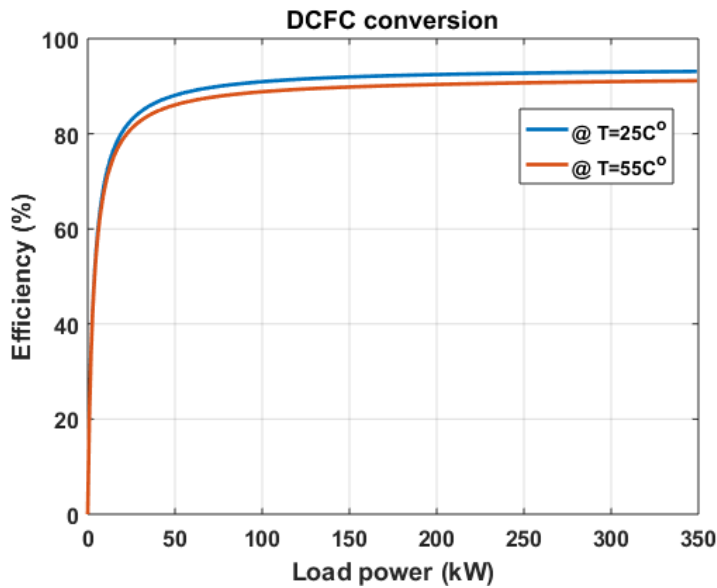


Figure 7. Estimated load-efficiency curves of 550-kVA PV conversion system.

For an ESS system, the commercial Schneider XCS40E 540-kVA Bidirectional Converter for ESS (Fig. 8), is considered. For a 2-MW ESS, four of these configurations (4×540 kVA) will be installed.

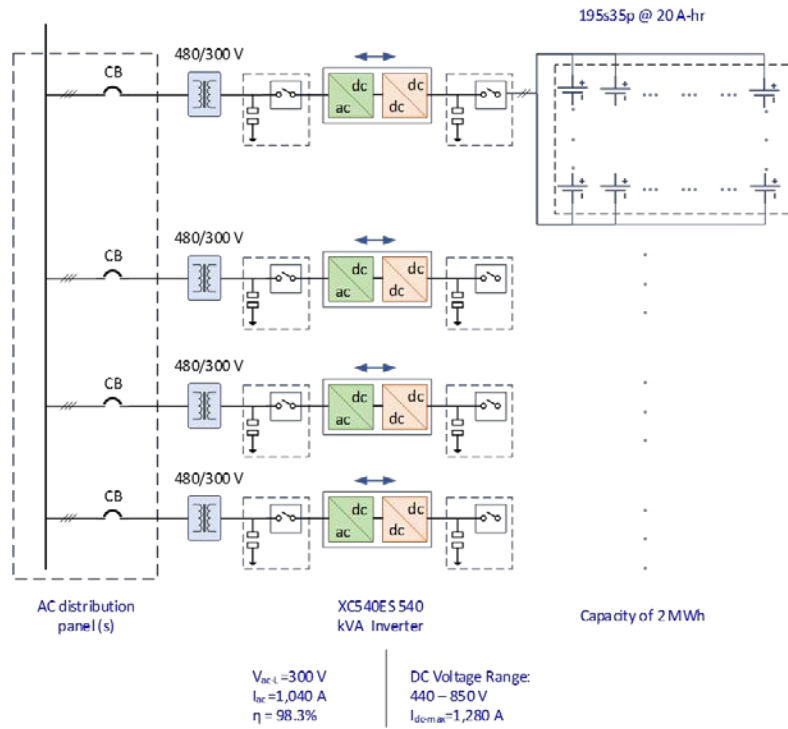


Figure 8. Schematic diagram of conventional ~2-MW ESS system.

A unique feature for the energy-conversion system of ESS is bidirectional conversion. The system is designed to charge (AC/DC) and discharge (DC/AC) to the ESS. For both charging and discharging operation, the system realizes different efficiency curves, which are presented in Figs. 9 and 10, respectively, for a 540-kW ESS.

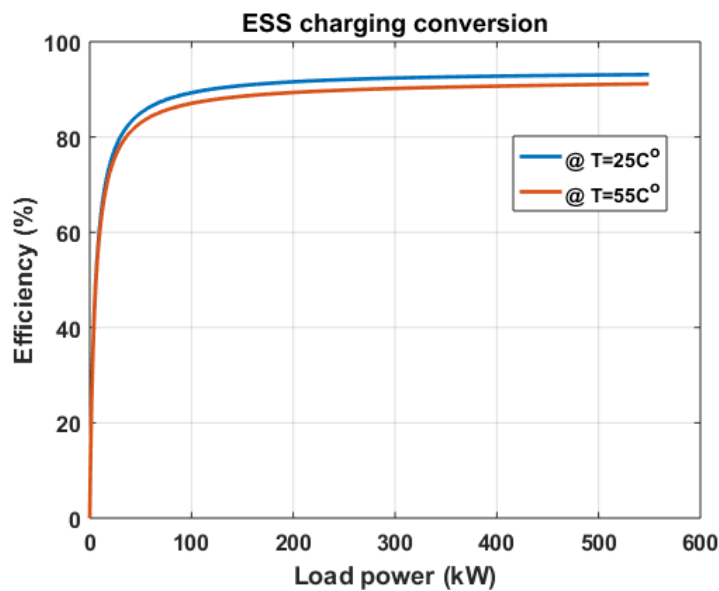


Figure 9. Estimated load-efficiency curves of 540-kVA ESS conversion system during charging.

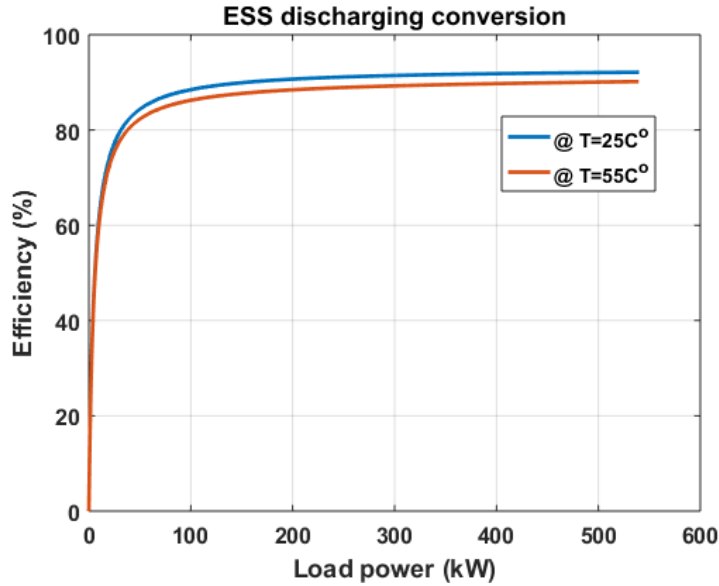


Figure 10. Estimated load-efficiency curves of 540-kVA ESS conversion system during discharging.

Conclusions

The team has begun integration discussion with the cost-analysis team on investigating the various power-conversion topologies (AC-coupled, DC-coupled, and multiple bus DC-coupled). The team expects to provide load-efficiency data (as look-up tables) for each configuration to the cost analysis team, to be integrated with the EnStore platform, considering the following variables: 1) load power, 2) charge/discharge operation, and 3) average ambient temperature. The estimation approach outlined above will support “datasheet” conversion efforts, although the team intends to leverage other activities to refine these models for actual equipment available in the ESIF. The task objectives for investigating the primary power conversion are expected to support a broader understanding—of which scenarios—based on energy throughput, onsite equipment, and more—will benefit from these new approaches to identify operational benefits.

BTMS Materials Development

Yeyoung Ha, Sang-Don Han, Kyusung Park (NREL), Andrew Jansen (ANL)

Background

To develop rechargeable battery systems suitable for the Behind-the-Meter Storage (BTMS), we are investigating $\text{Li}_4\text{Ti}_5\text{O}_{12}$ (LTO) anode and Mn-based cathode— LiMn_2O_4 (LMO), $\text{LiNi}_{0.5}\text{Mn}_{1.5}\text{O}_4$ (LMNO), and $\text{Li}_2\text{MnO}_3\text{-LiMO}_2$ —systems operating at 45 °C. In Q1 FY20, thorough examinations of new electrolyte systems involving a variety of Li salt and solvent combinations were performed, focusing on their anodic stability, half-cell performance, and full-cell performance. Among the electrolytes tested, lithium hexafluorophosphate (LiPF_6) in propylene carbonate (PC) and lithium tetrafluoroborate (LiBF_4) in PC showed promising results. This quarter, LiPF_6/PC and LiBF_4/PC systems were further interrogated by including ethylene carbonate (EC) as a co-solvent, because previous studies have shown enhanced ionic conductivity of the electrolyte when EC is added to PC.¹

Results

LTO, LMO, and LMNO electrodes were provided by the CAMP facility at ANL. Detailed information of each electrode is listed in Table 1. LTO/LMO and LTO/LMNO full cells were assembled in 2032-type coin-cell configuration using different electrolyte combinations. Four different electrolytes (1 M of LiPF_6 or LiBF_4 in PC or fluoroethylene carbonate (FEC)) were examined. The cycle performance of coin cells at 45 °C was tested using the following electrochemical protocol: 6 h rest at the open-circuit voltage (OCV) → 2 formation cycles at C/10 → 1,000 aging cycles at 1C. 1.5–3.0 V and 1.5–3.5 V cutoff voltages were used for LTO/LMO and LTO/LMNO cells, respectively. The results are presented in Figure 1.

For LTO/LMO cells, PC-based electrolytes showed better performance (i.e., higher capacity retention and higher coulombic efficiency) than the FEC-based electrolytes and the conventional Gen2 electrolyte (1.2 M LiPF_6 in EC/EMC (3:7, wt/wt)). Both LiPF_6/PC and LiBF_4/PC exhibited ~80% capacity retention by the 1000th cycle. Although the cycle performance of LTO/LMO cells showed a solvent-dependent trend, that of the LTO/LMNO cells showed a salt-dependent trend—where LiBF_4 -based electrolytes showed superior performance to the LiPF_6 -based electrolytes. All LiPF_6 -based electrolytes, including Gen2, exhibited rapid capacity fade in LTO/LMNO cells. Comparing the two LiBF_4 -based electrolytes, LiBF_4/PC showed a higher discharge capacity and better capacity retention initially, but the cell started to fade quickly after ~400 cycles. Such behavior may be correlated to the low coulombic efficiency of LiBF_4/PC electrolyte.

Table-1. Electrodes Examined in this Report

	Specifics
$\text{Li}_4\text{Ti}_5\text{O}_{12}$ (LTO)	- 87 wt% Samsung $\text{Li}_4\text{Ti}_5\text{O}_{12}$ + 5 wt% Timcal C45 + 8 wt% Kureha 9300 PVDF - Single-side coating on 20- μm Al foil - Coating thickness of 102 μm ; Porosity 55.6%; Loading 14.20 mg/cm^2 ; Density 1.38 g/cm^3
LiMn_2O_4 (LMO)	- 90 wt% Toda LiMn_2O_4 + 5 wt% Timcal C45 + 5 wt% Solvay 5130 PVDF - Single-side coating on 20- μm Al foil - Coating thickness of 76 μm ; Porosity 33.5%; Loading 18.86 mg/cm^2 ; Density 2.48 g/cm^3
$\text{LiNi}_{0.5}\text{Mn}_{1.5}\text{O}_4$ (LMNO)	- 84 wt% $\text{LiMn}_{1.5}\text{Ni}_{0.5}\text{O}_4$ + 8 wt% Timcal C45 + 8 wt% Solvay 5130 PVDF - Single-side coating on 20- μm Al foil - Coating thickness of 62 μm ; Porosity 33.8%; Loading 14.88 mg/cm^2 ; Density 2.40 g/cm^3

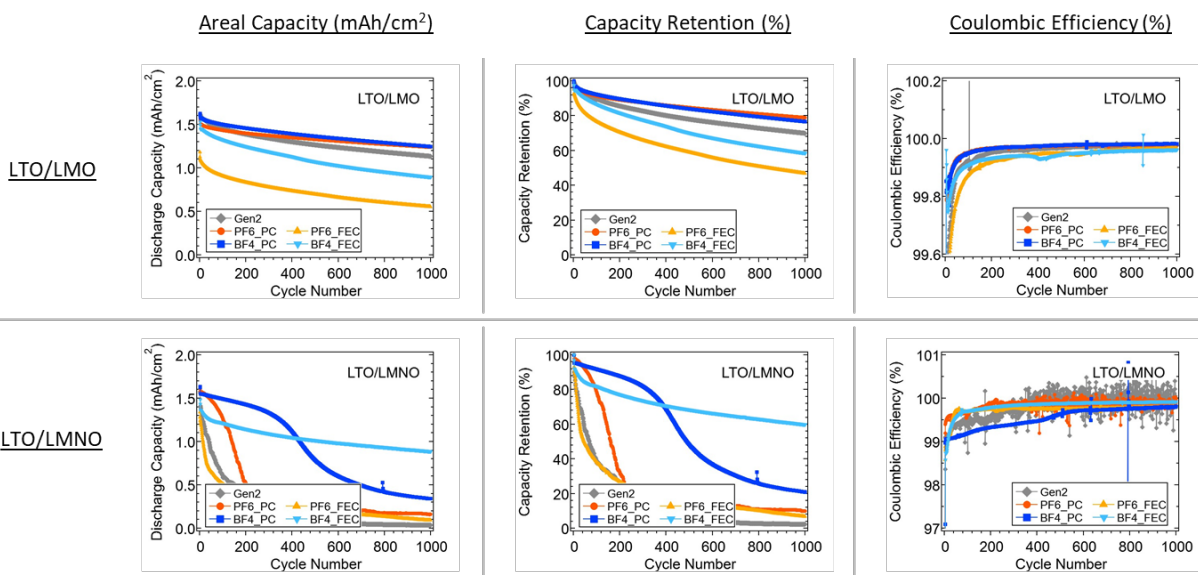


Figure 3. Cycle performance of LTO/LMO (top row) and LTO/LMNO (bottom row) cells with LiPF_6 and LiBF_4 in PC and FEC electrolytes. Gen2 electrolyte is shown as comparison. Cells were cycled at C/10 for 2 formation cycles and at 1C for 1000 aging cycles. LTO/LMO cells were cycled between 1.5 and 3.0 V, and LTO/LMNO cells were cycled between 1.5 and 3.5 V.

Previously, Ding and Jow reported a linear increase of the ionic conductivity of LiBF_4/PC and LiPF_6/PC electrolytes as EC is mixed with PC (up to 60 wt%).¹ Because PC-based electrolytes showed good cycle performance for LTO/LMO and LTO/LMNO cells, EC-PC binary solvent systems were investigated. EC and PC were mixed in 100:0, 75:25, 50:50, 25:75, and 0:100 ratios by weight. The results for LiBF_4 - and LiPF_6 -based electrolytes are presented in Figs. 2 and 3, respectively. LiBF_4 -based electrolytes were tested for both LTO and LMO cathodes, and LiPF_6 -based electrolytes were tested only for LMO because LiPF_6/PC showed poor performance for the LTO/LMNO cell.

In Fig. 2, LTO/LMO cells cycled in a series of $\text{LiBF}_4/\text{EC-PC}$ electrolytes all showed similar capacity retention and coulombic efficiency. For LTO/LMNO cells, adding EC to PC resulted in worse capacity retention, although the coulombic efficiency remained similar. None of the LTO/LMNO cells tested so far was able to maintain capacity retention over 80% for more than ~300 cycles, so this system may not be the choice for BTMS applications. To use such high-voltage cathodes, new electrolyte systems will need to be developed.

$\text{LiPF}_6/\text{EC-PC}$ electrolytes tested with LTO/LMO cells showed similar discharge capacity upon cycling (Fig. 3). However, 100% EC electrolyte showed the highest coulombic efficiency among all solvent combinations. Moreover, having more EC in the solvent reduced the overpotential in the voltage profiles and dQ/dV plots. Because EC has a higher viscosity than PC, having a more facile kinetics (i.e., smaller overpotential) in the 100% EC electrolyte may seem counterintuitive. Nonetheless, assuming that the linear increase of ionic conductivity at higher EC content continues beyond the point presented in the aforementioned literature (60 wt%), then it is possible that the gain in the ionic conductivity will compensate for the loss in the viscosity. In addition, EC may have a positive impact on other factors that affect the cell performance. For example, if EC forms a more favorable cathode/electrolyte interface (CEI) than PC, then the resistance will be reduced at the electrode/electrolyte interface and the overpotential will be smaller.

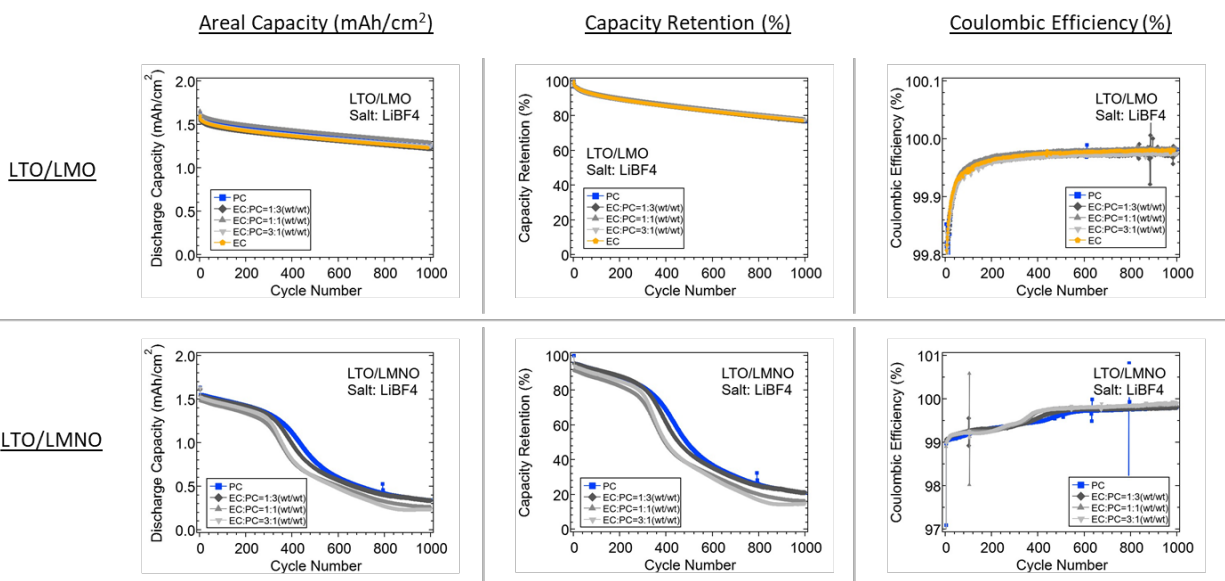


Figure 4. Cycle performance of LTO/LMO (top row) and LTO/LMNO (bottom row) cells with LiBF₄ salt in a series of EC-PC solvent mixtures. Cells were cycled at C/10 for 2 formation cycles and at 1C for aging cycles. LTO/LMO cells were cycled between 1.5 and 3.0 V, and LTO/LMNO cells were cycled between 1.5 and 3.5 V.

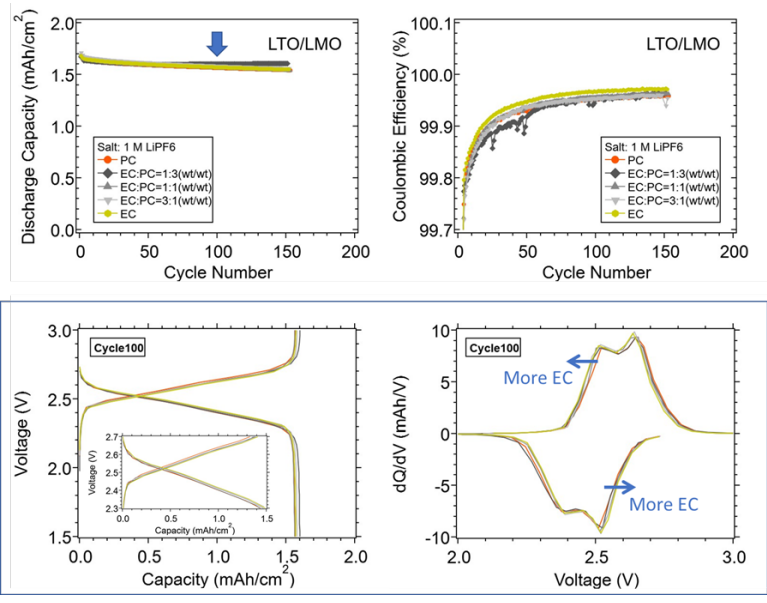


Figure 5. Cycle performance of LTO/LMO cells with LiPF₆ salt in a series of EC-PC solvent mixtures (top row). Cells were cycled at C/10 for 2 formation cycles and at 1C for aging cycles between 1.5 and 3.0 V. Voltage profiles and dQ/dV plots of the 100th cycle in each system are shown in the bottom row.

Conclusions

EC and PC binary solvent systems were investigated to develop electrolytes with higher ionic conductivity, targeting the use of thick electrodes. LiBF₄ and LiPF₆ salts, which showed good cycle performance in PC solvents, were tested for LTO/LMO and LTO/LMNO cells. No dramatic change in the cycle performance was observed when EC was added to PC in different ratios. But the kinetics were enhanced for the LTO/LMO cells tested with LiPF₆-based electrolytes when the EC content was higher. Also, note that the electrodes tested here are less than 100 μm thick, and different behavior may be observed when thicker electrodes are tested. These results with thinner electrodes serve as a good baseline, showing that there is no compatibility issue among the constituents. As next steps, we will test the electrolyte properties, such as ionic conductivity and viscosity, at varying temperatures to understand the source of enhanced kinetics at higher EC ratio. Different EC:PC ratios and salt concentrations will be examined. Also, we will continue the electrolyte development with thicker electrodes. Finally, we will test symmetric cells under different conditions (e.g., cycled vs. not cycled counter electrode, different cathode and electrolyte combinations) to interrogate the failure mechanisms of the cells.

References

1. Ding, M. S.; Jow, T. R., How Conductivities and Viscosities of PC-DEC and PC-EC Solutions of LiBF₄, LiPF₆, LiBOB, Et₄NBF₄, and Et₄NPF₆ Differ and Why. *J. Electrochem. Soc.* **2004**, *151*, A2007-A2015.
-